

## Foil Black Hole Foils: Revealing Horizon Alternatives with Baryonic Atmospheres

SHOKOUFE FARAJI<sup>1,2,3</sup> AND AVERY E. BRODERICK<sup>3,1,2</sup>

<sup>1</sup>Department of Physics and Astronomy, University of Waterloo, 200 University Avenue West, Waterloo, ON, N2L 3G1, Canada

<sup>2</sup>Waterloo Centre for Astrophysics, University of Waterloo, Waterloo, ON N2L 3G1 Canada

<sup>3</sup>Perimeter Institute for Theoretical Physics, 31 Caroline Street North, Waterloo, ON, N2L 2Y5, Canada

### ABSTRACT

Event horizons are a defining feature of black holes. Consequently, there have been many efforts to probe their existence in astrophysical black hole candidates, spanning ten orders of magnitude in mass. Nevertheless, horizons remain an obstacle to unifying general relativity and quantum mechanics, most sharply presented by the information paradox. This has motivated a proliferation of horizonless alternatives (black hole foils) that avoid event horizons and are therefore benign. We show that for typical accreting astronomical targets, largely independent of a foil’s underlying microphysics, a horizonless compact surface will generically be ensconced within an optically thick, scattering dominated baryonic settling layer that efficiently reprocesses the kinetic energy of infalling matter into observable thermal emission. The emergent photosphere luminosity is driven toward the accretion-powered equilibrium value and is only weakly sensitive to the foil redshift. These atmospheres are convectively stable and naturally imply that the emitting photosphere forms at modest redshift even when the surface redshift is extreme. Moreover, local gas-surface interaction provides a microphysical lower bound on the effective base temperature, insulating the atmosphere from arbitrarily cold foils. The unknown properties of the foil enter only through local boundary conditions controlling baryon processing and thermal coupling at the surface, making the solutions broadly applicable to horizonless alternatives that do not invoke significant additional nonlocal interactions. Thus, under minimal assumptions (GR exterior and local surface interactions), horizonless foils are generically observationally exposed: the absence of a thermal photosphere directly constrains or rules out broad classes of such models.

**Keywords:** Gravitation, Naked singularities, Radio continuum emission, High energy astrophysics, Galactic center, Active galaxies, Strong gravitational lensing

### 1. INTRODUCTION

With the advent of direct near-horizon probes, via gravitational waves (Abbott et al. 2016; Abac et al. 2025) or direct imaging (Event Horizon Telescope Collaboration et al. 2019a, 2022a), the study of black hole horizons<sup>1</sup>

has become an empirical effort. Nevertheless, black hole horizons remain a significant theoretical impediment to the long sought unification of general relativity and quantum mechanics, often described via the information paradox and its cousins (Hawking 1976; Preskill

1992; Mathur 2009; Almheiri et al. 2013). One way that these conceptual concerns can be retired is to simply avoid the existence of black hole horizons altogether, i.e., do away with black holes and replace them with some object that is causally connected to the external universe (Mathur 2002; Mathur & Mehta 2024).

While significant effort has been devoted to deriving horizon-scale modifications from candidate microscopic theories or controlled semiclassical frameworks – including string-theoretic microstate geometries/fuzzballs (Mathur 2005; Skenderis & Taylor 2008; Bena & Warner 2007; Warner 2019; Bena & Warner 2025), horizonless ultracompact solutions in asymptotically free quadratic gravity (Holdom & Ren 2017), and semiclassical backreaction models (Barceló et al. 2008; Arrechea et al. 2022) – explicit solutions that are demonstrably generic, dynamically formed, and astrophysically complete remain limited.

In contrast, a broad class of black hole foils, typically qualitatively motivated alternatives that avoid an event horizon by introducing novel,

<sup>1</sup> The teleological definition of the event horizon renders it operationally subtle as an empirical object. Nevertheless, Hawking-like particle creation does not require a global event horizon; a slowly evolving apparent/trapping horizon (or, more generally, an approximately exponential redshift relation between  $\mathcal{I}^-$  and  $\mathcal{I}^+$ ) is sufficient (Visser 2003; Barceló et al. 2011). therefore we focus our attention on what we might call “astrophysical” horizons, i.e., objects that look like black holes on astronomically relevant timescales. It is to these that we shall refer to as horizons henceforth.

often unknown, physics (e.g., gravastars (Mazur & Mottola 2004; Visser & Wiltshire 2004), ultracompact fluid configurations tied to Buchdahl-type limits (Buchdahl 1959; Danielsson & Giri 2021), boson stars (Kaup 1968; Ruffini & Bonazzola 1969; Liebling & Palenzuela 2012); see also the review (Cardoso & Pani 2019)). Because the information paradox would arise should a black hole horizon exist anywhere in the universe, such programs must imagine replacing the entire mass range of observed black hole candidates, from roughly  $5 M_\odot$  to  $7 \times 10^9 M_\odot$  (Abac et al. 2024; Event Horizon Telescope Collaboration et al. 2019b). Therefore, even absent an underlying fundamental theory, black hole foils are useful parameterizations of the observational constraints on the existence of black hole horizons, hence their name.

Over the past quarter century, a class of arguments for the observational existence of black hole horizons based on accreting black hole candidate systems has been proposed (Narayan et al. 1997; Narayan & Heyl 2002; McClintock et al. 2004; Broderick & Narayan 2007; Narayan & McClintock 2008; Broderick et al. 2009, 2015). Essentially, these invoke the possibility of an observable thermal photosphere powered by the kinetic energy within the accretion flow as it plunges onto the black hole foil. In steady state, the luminosity measured at infinity from a thermal photosphere,

$$A_\infty \sigma T_\infty^4 \approx \eta \dot{M} c^2, \quad (1)$$

is balanced by the incoming accretion power, where  $A_\infty$ ,  $T_\infty$ , and  $\dot{M}$  are the apparent photosphere area, temperature, and mass accretion rate as measured by an observer at infinity,  $\sigma$  is the Stefan-Boltzmann constant, and  $\eta \sim 0.5$  is an efficiency factor describing the kinetic energy still held by the accreting matter as it plunges into the photosphere. Very compact surfaces, i.e., black hole foils with high surface redshifts, simplify the argument via the strong gravitational lensing that serves to couple the surface to itself, facilitating thermalization. The presence of such photospheres has been excluded at overwhelming confidence in the two horizon-scale Event Horizon Telescope targets, M87\* and Sgr A\* (Event Horizon Telescope Collaboration et al. 2019b, 2022b; Broderick et al. 2023). The remaining debate centers on when and if a given black hole foil might develop a thermally emitting surface.

Unfortunately, due to their poorly defined nature, the physical properties of black hole foil surfaces are inherently difficult to generally assess. For example, some foils invoke near-infinite heat capacities and near-zero surface temperatures, and thus seek to evade the observational constraints by never reaching steady state between the thermal surface luminosity and kinetic power

of the accreting matter.<sup>2</sup> However, these complications could be avoided if the photosphere was a feature of the accretion flow itself, which is comprised of well understood baryonic matter and electromagnetic fields. Such a simplification was instrumental in recent constraints on the existence of naked singularities

(Vieira & Klužniak 2023; Broderick & Salehi 2024). Where there it was motivated by the particular gravitational properties of curvature singularities, here it is a natural consequence of the collection and relaxation of the accreting matter within the boundary layer of the settling flow.

In constructing a suitable baryonic atmosphere around arbitrary black hole foils, we make a pair of key assumptions:

1. Gravity may be well described outside of the foil surface by general relativity.
2. Any novel interactions between the accreting baryonic matter and the surface must be (nearly) local, i.e., they must occur within an appropriate “small” distance of the surface.

The former appears well established, at least to order unity, by gravitational wave observations (Abbott et al. 2025) and direct imaging (Kocherlakota et al. 2021; Event Horizon Telescope Collaboration et al. 2022b; Broderick et al. 2023). The latter may very well not be true, but deviations from locality are capable of solving the information paradox without the need for foils altogether, and thus form a separate class of solution.<sup>3</sup> We also adopt spherical symmetry for computational simplicity, but do not anticipate this to be a significant qualitative restriction. The properties of the black hole foil are distilled into two local pieces of boundary data: one controlling the inward baryon flux (a mass transmittance parameter) and one controlling the exchange of heat at the surface (an energy exchange condition expressed through the base temperature).

In this way, we construct a widely applicable set of astrophysical models of a well-behaved thermal photospheres that envelop and thereby reveal black hole foils, independent of the specific underlying physical mechanisms responsible for avoiding the appearance of a horizon.

Specifically, we construct a minimal relativistic model of a steady, spherically symmetric, subsonic baryonic settling layer (atmosphere) between an outer photo-

<sup>2</sup> It is of interest that wherein a suitable microphysical model is provided, it may be possible to exclude these, e.g., Broderick & Narayan (2007). It would seem, therefore, that this lack of definition may be a “feature”, though one that should be challenged.

<sup>3</sup> While it certainly remains possible that physics deviates simultaneously in multiple ways from the standard picture near black hole candidates, we view this as a doubly extraordinary solution, and focus on the more ordinary singly extraordinary possibilities.

sphere and a physical surface (foil) supported by internal pressure gradients. Energy is transported through the atmosphere by radiative diffusion, while mass is carried by slow subsonic settling, subject to boundary conditions at an outer accretion shock (where power and momentum are supplied) and at the foil surface.

We explicitly derive the radiative diffusion law (and thus conservation of luminosity as seen by observers at infinity) from a stress-energy conservation and the associated timelike Killing current. In appendices, we discuss the physical origins of opacity within the atmosphere and

explore a variety of modifications to the simplest picture, incorporating radiation pressure and inertia, various radiative transfer processes, and relaxing the slow-settling condition; we find that in all cases the photosphere luminosity remains close to the steady state, accretion powered value for optically thick atmospheres.

Therefore, this framework provides a controlled way to assess whether redshift and diffusion can hide accretion power in surface atmospheres and thus places sharp, transparent constraints on horizonless alternatives. The paper is organized as follows: Section 2 states equations of atmospheric structure and assumptions. Section 3 presents the nonrelativistic equations for intuition, followed by the full relativistic system, its rationalized formulation, and approximate solutions in the compact surface limit in Section 4. We then state the boundary/viability conditions, microphysical base condition and the resulting bounds in Section 5. Section 6 summarizes the results and conclusions.

## 2. ATMOSPHERIC STRUCTURE

We consider a horizonless compact object (a foil) with a material surface at radius  $r_f$ , whose exterior spacetime is well described by the Schwarzschild solution. Because accreting baryons do not disappear through a horizon, continuous supply naturally leads to the formation of a quasi-stationary boundary layer: a pressure-supported settling atmosphere extending from an outer photosphere (either an accretion shock or a smooth matching surface to the inflow) down to the foil. We adopt a minimal description in which the atmosphere is steady, spherically symmetric, and subsonic, with gas pressure providing the dominant support, and with radiative energy transport captured by diffusion through a layer that is geometrically thin yet optically thick. Under these assumptions the structure is determined by radial transport equations for mass, momentum, and energy, closed by boundary conditions at the outer photosphere (where the inflow supplies power and momentum) and at the foil surface (where the microphysics controls the exchange of mass and heat). In steady, spherically symmetric flow the interior solution is determined by first-order radial transport equations, so inner data must be specified at the foil to fix how mass and heat are exchanged; otherwise the problem is underdetermined and the interior

cannot be matched uniquely to the outer photosphere or shock. We therefore permit an extreme range of possibilities by setting:

1. Surface temperature  $T_f$ . This may differ substantially from the temperature of the accreting gas. For example, in gravastar models with very large heat capacity and even nearly infinite, one might have  $T_f \approx 0$  K.
2. Inward mass flux at the surface  $J_f$ . We adopt a linear closure with the density just above the surface,

$$J_f = r_f^2 \mathcal{T} \rho_f v_{\text{th}}, \quad (2)$$

where  $r_f$  is the surface radius,  $\rho_f$  the baryon density immediately above the surface,  $v_{\text{th}}$  a characteristic thermal speed, and  $\mathcal{T}$  a dimensionless surface transmission coefficient that encodes the microphysics of baryon absorption by (or conversion at) the foil. Such a mechanical picture turns out to be practically convenient.

Here and throughout,  $\rho_f \equiv \rho(r_f^+)$  and  $T_f \equiv T(r_f^+)$  denote the baryon density and gas temperature immediately outside the foil surface. The second condition allows the foil either to absorb the accreting baryons or to convert them into other forms of matter. We choose the sign convention that  $J_f > 0$  denotes inward mass flow. The form Equation 2 matches the conserved spherical mass flux used below: in steady flow  $J$  is constant with radius and equals  $J_f$  at the surface, with the convention that  $J > 0$  denotes inward accretion.<sup>4</sup>

We will also make the following simplifying assumptions, none of which we expect to be violated in practice, and many of which we are able to subsequently verify:

1. Steady state. Therefore we have  $\nabla_\mu(\rho u^\mu) = 0$  and the Killing energy flux is conserved ( $dL_\infty/dr = 0$ ). A posteriori this requires the supply timescale to exceed both the settling and diffusion times ( $t_{\text{sup}} \gg t_{\text{acc}}, t_{\text{diff}}$ ).
2. Spherical symmetry. Angular structure is neglected so all quantities depend only on  $r$ . Any residual rotation, magnetic stresses, or multipoles are assumed small enough to enter as higher-order corrections to the radial balance.
3. Slow (subsonic) settling.  $v^r \ll c$  and  $M \equiv |v^r|/c_s \ll 1$  with  $c_s^2 = kT/m$ . This ensures pressure support dominates, no sonic point forms in the atmospheric layer, and is consistent with the surface transmission bound  $|\mathcal{T}| < 1$  used below.

<sup>4</sup>  $[J_f] = MT^{-1}$ ; indeed,  $[r_f^2 \rho_f v_{\text{th}}] = L^2 \times ML^{-3} \times LT^{-1} = MT^{-1}$ . Angular factors and distribution function constants are absorbed into  $\mathcal{T}$ .

4. Photon pressure subdominant. The gas is ideal and baryon-dominated:  $P_{\text{rad}} \ll P_{\text{gas}}$  with

$$\frac{P_{\text{rad}}}{P_{\text{gas}}} = \frac{(1/3) a T^4}{\rho k T / m} = \frac{a m}{3k} \frac{T^3}{\rho} \ll 1, \quad (3)$$

where  $a = 4\sigma/c$ . We will monitor this ratio in the solutions to validate the closure.

5. Geometrically thin atmosphere. The scale height

$$H \equiv \frac{kT}{m|g|}, \quad |g(r)| = \frac{GM}{N(r)r^2}. \quad (4)$$

The pressure scale height satisfies  $H/r_f \ll 1$  (equivalently  $\Delta r \sim N_f H \ll r_f$ ). This permits evaluating geometric prefactors at  $r_f$  (e.g.  $r \simeq r_f$  outside derivatives) while retaining the exact lapse  $N(r)$ , whose variation can remain  $O(1)$  in the compact surface limit.

6. Exterior Schwarzschild geometry. Outside the foil the spacetime is static and spherically symmetric,

$$ds^2 = -N^2(r) dt^2 + N^{-2}(r) dr^2 + r^2 d\Omega^2, \quad (5)$$

where

$$N^2(r) = 1 - \frac{2GM}{rc^2}. \quad (6)$$

This is appropriate when rotation and frame dragging are negligible for the atmospheric layer; any such effects would appear as controlled corrections.

7. Optical thick. The radiative transport law used throughout is the diffusion limit and therefore requires that the atmosphere be optically thick on the local pressure support scale (more discussion in [Appendix A](#).)

### 3. NON-RELATIVISTIC LIMIT

We begin with the relevant equations in the non-relativistic limit, both as a comparison for the subsequent fully relativistic treatment and as a tool for building intuition about the resulting solution. The equations we utilize are the standard (nonrelativistic) stellar-structure equations specialized to the case without volumetric heating ( $dL/dr = 0$ ) (see, e.g., [Kippenhahn & Weigert \(1994\)](#)). Specifically, these are continuity

$$\frac{d}{dr} (r^2 \rho v^r) = 0, \quad (7)$$

the radial component of the Euler equation

$$\rho v^r \frac{d}{dr} v^r = -\frac{d}{dr} P + \rho g, \quad (8)$$

where  $P = \rho k T / m$  (ideal gas;  $m$  is the mean particle mass) and  $g$  is the gravitational acceleration, and the radiative diffusion equation

$$\frac{dT}{dr} = -\frac{3\kappa\rho L}{64\pi\sigma r^2 T^3}, \quad (9)$$

where  $\sigma$  is the Stefan-Boltzmann constant,  $L$  is the outward luminosity carried through a sphere of radius  $r$ , and  $\kappa$  is the (here taken constant) opacity, dominated by electron scattering <sup>5</sup>.

We do not supplement this with an energy generation equation ( $dL/dr = 4\pi r^2 \rho e$ ), since no volumetric heating is expected; therefore  $L$  is radially constant and is fixed by the boundary condition at the photosphere/shock. At the accretion shock or matching photosphere located at  $r_s$ , we take

$$L = 4\pi r_s^2 \sigma T_s^4 - \eta \dot{M} c^2, \quad (10)$$

with the first term the outward blackbody surface luminosity and the second the inward accretion power (so typically  $L < 0$ ). With this sign convention a negative  $L$  implies  $\partial_r T > 0$  by [Equation 9](#); i.e., the temperature rises outward across the atmosphere, rendering the layer convectively stable (via the Schwarzschild criterion, CITE). The observed surface luminosity is the outward term,  $L_{\text{surf}} = 4\pi r_s^2 \sigma T_s^4$ , while the net energy flux through the atmosphere is  $L$  (usually negative in the accretion-powered case).

In addition, continuity implies that  $J \equiv r^2 \rho v^r$  is constant and simultaneously set by the conditions at the accretion shock and the foil surface,

$$J = \frac{\dot{M}}{4\pi} = r_f^2 \mathcal{T} \rho_f \sqrt{\frac{kT_f}{m}}. \quad (11)$$

Thus we have a boundary condition on the atmosphere density,

$$\rho_f = \frac{\dot{M}}{4\pi r_f^2 \mathcal{T} \sqrt{kT_f/m}}. \quad (12)$$

The radial Euler equation may be reconfigured to remove  $v^r = J/(r^2 \rho)$ . Using the thin layer approximation  $r \simeq r_f$  (so  $r$  dependences outside derivatives are evaluated at  $r_f$ ), and writing  $dP/dr = (k/m)(T d\rho/dr + \rho dT/dr)$  and substituting  $v^r = J/(r_f^2 \rho)$  into  $\rho v^r dv^r/dr$ ; then inserting the diffusion law [Equation 9](#), yields

$$\frac{d\rho}{dr} \approx \rho \frac{\frac{g}{kT} + \frac{3k\kappa\rho L}{64\pi r_f^2 m \sigma T^3}}{\frac{J^2}{m} - \frac{J^2}{r_f^4 \rho^2}}. \quad (13)$$

The outward luminosity  $L$  is negative in the accretion powered case, and  $g = -GM/r^2 < 0$ , so both terms in the numerator are negative. The denominator in [Equation 13](#) is the usual sonic discriminant: it approximately reduces to  $c_s^2 - (v^r)^2$  with  $c_s^2 = kT/m$ . Because the settling flow is subsonic by assumption, the denominator

<sup>5</sup> [Equation 9](#) is the standard form  $\frac{d}{dr} T = -(3\kappa\rho L)/(16\pi acr^2 T^3)$  rewritten using  $ac = 4\sigma$ .

is positive. Therefore  $\rho(r)$  decreases monotonically with radius and, correspondingly,  $v^r$  increases monotonically.

This condition places a natural constraint on  $\mathcal{T}$  at  $r_f$ :

$$\frac{kT}{m} - \frac{J^2}{r_f^4 \rho_f^2} = \frac{kT_f}{m} (1 - \mathcal{T}^2) > 0 \Rightarrow |\mathcal{T}| < 1. \quad (14)$$

Combined, [Equation 9](#) and [Equation 13](#) define an initial value problem given  $(\rho_f, T_f)$ ; the equations may be integrated outward until the outer boundary condition is satisfied. While [Equation 10](#) fixes the net luminosity, we still require the shock (photosphere) radius  $r_s$ . The latter is set by the jump conditions; a useful estimate is

$$P_s \approx \frac{\dot{M}c}{4\pi r_s^2}, \quad (15)$$

i.e., the post shock pressure balances the ram pressure  $\rho_a u_a^2$  with  $4\pi r_s^2 \rho_a u_a = \dot{M}$  and  $u_a \sim c$  near the shock.

### 3.1. Characteristics of Solutions

Even without strong field corrections, the nonrelativistic (NR) limit already fixes the qualitative architecture of any steady, pressure supported settling layer. It yields two robust predictions that do not depend on micro-physics: (i) the sonic discriminant at the base must remain positive (no hidden sonic point), and (ii) when the net luminosity  $L \leq 0$  the pressure profile is strictly decreasing. Both statements survive verbatim in the relativistic treatment once the redshift factors  $N(r)$  are restored; only coefficients change. These NR results therefore provide clean, model independent diagnostics that we will carry forward.

First, if the denominator of [Equation 13](#) is negative, the density gradient becomes positive and the configuration loses pressure support at the base (the flow there is supersonic). We therefore require

$$\sqrt{\frac{kT_f}{m}} > v_f^r = \frac{J}{r_f^2 \rho_f}. \quad (16)$$

Second, the pressure gradient is generically negative throughout the subsonic settling layer. Starting from Euler,

$$\frac{dP}{dr} = \rho g + (v^r)^2 \frac{d\rho}{dr}, \quad v^r = \frac{J}{r_f^2 \rho}, \quad (17)$$

and substituting [Equation 13](#) (with the thin-layer approximation  $r \simeq r_f$ ) gives

$$\frac{dP}{dr} = \frac{\rho \frac{kT}{m} g + \frac{3k\kappa L}{64\pi\sigma r_f^2 m T^3} \frac{J^2}{r_f^4}}{\frac{kT}{m} - \frac{J^2}{r_f^4 \rho^2}}. \quad (18)$$

The substitution cancels only the  $g(v^r)^2$  piece generated by the inertial term, leaving the expected hydrostatic

contribution (and recovering  $dP/dr \simeq \rho g$  when  $(v^r)^2 \ll kT/m$ ). For accretion-powered cases  $L \leq 0$  and  $g < 0$ , while the denominator is positive in the subsonic regime, so  $dP/dr < 0$  throughout the settling layer.

A direct consequence is that the pressure at the base must exceed the post shock pressure; otherwise the outer jump conditions cannot be satisfied. Using the standard ram-pressure estimate at the shock [Equation 15](#), we require

$$P_f > P_s \implies \rho_f \frac{kT_f}{m} > \frac{\dot{M}c}{4\pi r_s^2} \simeq \frac{\dot{M}c}{4\pi r_f^2}, \quad (19)$$

where in the last step we used  $r_s \simeq r_f$  (Order unity factors in the shock jump can be absorbed in this estimate; the inequality is the key requirement.).

### 3.2. Approximate Solution

To expose the dominant scalings, we now construct an approximate solution in a regime where the temperature varies only weakly across one scale height and the base flow is strongly subsonic. Concretely, we assume:

1. Weak temperature variation across  $H$ . This is the precise condition that allows us to treat  $T$  as approximately constant when solving the hydrostatic balance.
2. Strong pressure support at the base. The flow is strongly subsonic there:  $c_s \gg v^r$ , i.e.,  $kT_f/m \gg J^2/(r_f^4 \rho^2)$ .

Density profile over the height scale: the consequence of the first one is temperature varies only weakly across a scale height ( $T$  nearly constant), while the density adjusts rapidly. Taking  $T \simeq \bar{T}$  constant in the hydrostatic term,

$$\frac{dP}{dr} = \rho g, \quad P = \frac{\rho k \bar{T}}{m}, \quad (20)$$

gives

$$\frac{d\rho}{dr} \simeq \rho \frac{mg}{k\bar{T}} \Rightarrow \rho(r) \simeq \rho_f \exp \left[ -\frac{(r - r_f)}{H} \right], \quad (21)$$

where  $H$  is given by [Equation 4](#). Thus, the density falls exponentially over the height scale  $H$ .

Temperature profile over the height scale: Inserting  $\rho \simeq \bar{\rho}$  (a layer average) into the diffusion equation, taking  $r \simeq r_f$ , multiplying by  $4T^3$  and integrating across one scale height gives

$$T_s^4 \simeq T_f^4 \left[ 1 - \frac{3\bar{\tau}L}{16\pi r_f^2 \sigma T_f^4} \right], \quad (22)$$

where  $\bar{\tau} \equiv \kappa \bar{\rho} H$  is the optical depth across one scale height. Because accretion power drives  $L \leq 0$  (outward positive), the bracket exceeds unity and  $T$  rises outward consistent with unconditional convective stability.

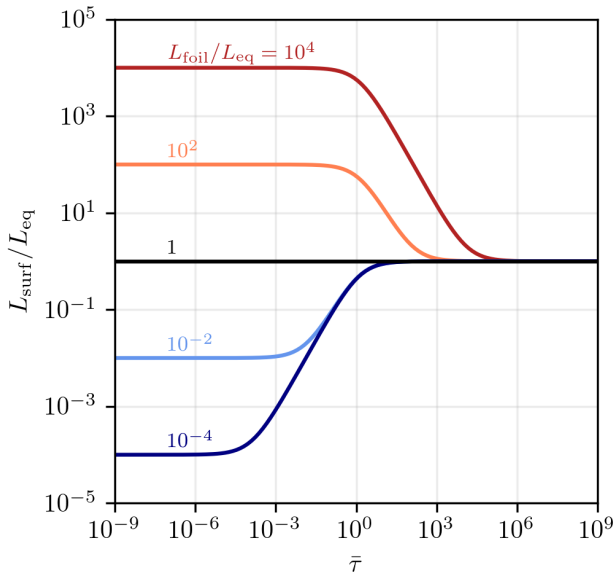


**Figure 1.** Surface luminosity at the top of the baryonic atmosphere as a function of atmosphere optical depth across one scale height for various foil luminosities. Curves correspond to different intrinsic foil luminosities  $L_{\text{foil}}/L_{\text{eq}}$  (labels). In the optically thin limit  $\bar{\tau} \ll 1$ , the layer is transparent and  $L_{\text{surf}} \simeq L_{\text{foil}}$ . In the optically thick limit  $(3/4)\bar{\tau} \gg 1$ , diffusion forces the emergent luminosity to  $L_{\text{surf}} \rightarrow L_{\text{eq}}$ , essentially independent of  $L_{\text{foil}}$ .

Surface luminosity: with  $L_{\text{surf}} \equiv 4\pi r_s^2 \sigma T_s^4 \simeq 4\pi r_f^2 \sigma T_s^4$  and  $L = L_{\text{surf}} - \eta \dot{M} c^2$ , Equation 22 yields

$$L_{\text{surf}} \simeq \frac{L_{\text{foil}} + \frac{3}{4} \bar{\tau} \eta \dot{M} c^2}{1 + \frac{3}{4} \bar{\tau}}, \quad (23)$$

where  $L_{\text{foil}} \equiv 4\pi r_f^2 \sigma T_f^4$ . Equation 23 shows that the photospheric luminosity is controlled by a single dimensionless parameter,  $(3/4)\bar{\tau}$ . This parameter characterizes how effectively radiation is retained and reprocessed within one pressure scale height before escaping. In the strongly optically thick regime,  $(3/4)\bar{\tau} \gg 1$ , the surface luminosity is driven to the accretion-powered equilibrium value  $L_{\text{surf}} \rightarrow \eta \dot{M} c^2 \equiv L_{\text{eq}}$ , essentially independent of the foil temperature. In the opposite regime,  $(3/4)\bar{\tau} \ll 1$ , the atmosphere cannot efficiently communicate the accretion power to the photosphere and the emergent luminosity relaxes toward the intrinsic foil luminosity  $L_{\text{surf}} \rightarrow L_{\text{foil}}$ . Figure 1 illustrates this interpolation for several values of  $L_{\text{foil}}/L_{\text{eq}}$ .

Using the surface boundary condition

$$\rho_f = \frac{\dot{M}}{4\pi r_f^2 \mathcal{T} v_{\text{th},f}}, \quad (24)$$

given

$$v_{\text{th},f} \equiv \sqrt{k T_f / m}, \quad (25)$$

and  $H$  is given by Equation 4, we obtain

$$\bar{\tau} \approx \frac{\kappa \dot{M}}{4\pi \mathcal{T} G M} \frac{k \bar{T} / m}{v_{\text{th},f}} = \frac{\kappa \dot{M}}{4\pi \mathcal{T} G M} \frac{c_s^2(\bar{T})}{v_{\text{th},f}}. \quad (26)$$

The approximation is self-consistent when

$$\varepsilon_T \equiv \frac{3 \bar{\tau} |L|}{16 \pi r_f^2 \sigma T_s^4} \ll 1, \quad (27)$$

i.e., when the fractional change in  $T^4$  across one scale height is small. In this regime the temperature is nearly constant over  $H$  and the optical depth  $\bar{\tau} \gtrsim 1$ , so our use of a single characteristic temperature and density within the layer is justified. Equations (23)-(26) then quantify precisely when the surface radiates at  $\eta \dot{M} c^2$  and when it relaxes toward  $L_{\text{foil}}$  for  $(3/4)\bar{\tau} \ll 1$ ; this is the small  $\bar{\tau}$  limit of this diffusion-based estimate. In particular, for fixed  $\bar{\tau}$  the condition  $\varepsilon_T \ll 1$  corresponds to the near equilibrium branch in which the net luminosity through the layer satisfies  $|L| \ll L_{\text{eq}}$ .

### 3.3. Rationalized Form

For explicit computations and to facilitate direct comparison with the relativistic case, we present a rationalized version of the equations of atmospheric structure that emphasizes the characteristic aspects of the above solutions. We define

$$\bar{x} = \rho / \rho_f, \quad (28a)$$

$$\bar{y} = T / T_{\text{eq}}, \quad (28b)$$

$$s = (r - r_f) / h, \quad (28c)$$

where the NR scale height at the equilibrium temperature is

$$h \equiv \frac{k T_{\text{eq}}}{m |g|}, \quad (29)$$

and

$$L_{\text{eq}} \equiv 4\pi r_s^2 \sigma T_{\text{eq}}^4 = \eta \dot{M} c^2. \quad (30)$$

we take  $r_s \simeq r_f$  within the thin layer. We also introduce the optical depth per height scale parameter

$$\tau_h \equiv \kappa \rho_f h. \quad (31)$$

Using the thin-layer approximation  $r \simeq r_f$  in the coefficients, the dimensionless equations become

$$\partial_s \bar{x} = \bar{x} \frac{-1 + \frac{3 \tau_h L}{16 L_{\text{eq}}} \frac{\bar{x}}{\bar{y}^3}}{\bar{y} - \mathcal{T}^2 \frac{\bar{y}_f}{\bar{x}^2}}, \quad (32a)$$

$$\partial_s \bar{y} = - \frac{3 \tau_h L}{16 L_{\text{eq}}} \frac{\bar{x}}{\bar{y}^3}, \quad (32b)$$

where the  $-1$  in the numerator of  $\partial_s \bar{x}$  is the (dimensionless) hydrostatic term  $hg/(kT_{\text{eq}}/m) = -1$ , and the coefficient follows from the NR diffusion law with  $ac = 4\sigma$  (hence the 16).

The boundary conditions are

$$\bar{x}_f = 1, \quad (33a)$$

$$\bar{y}_f = T_f/T_{\text{eq}}, \quad (33b)$$

$$\bar{x}_s \bar{y}_s = \frac{m}{\rho_f k T_{\text{eq}}} \frac{\dot{M} c}{4\pi r_s^2} = \left(\frac{r_f}{r_s}\right)^2 \frac{\mathcal{T} c}{\sqrt{|g|} h} \bar{y}_f^{1/2}, \quad (33c)$$

$$L = L_{\text{eq}} (\bar{y}_s^4 - 1), \quad (33d)$$

where we used  $J = \dot{M}/(4\pi) = r_f^2 \mathcal{T} \rho_f \sqrt{k T_f/m}$  in the second equality of the third line. The shock/outer pressure condition enters via  $\rho_s (k T_s/m) \simeq \dot{M} c / (4\pi r_s^2)$ . Further,  $L$  is radially constant in the layer, fixed by the outer boundary condition.

#### 4. RELATIVISTIC LIMIT

Because the atmospheric layer lies at high redshift ( $N \ll 1$ ), and therefore relativistic effects control the dynamics. Nevertheless, we pursue an analogous path as in the NR derivation but work with the proper variables ( $\rho, u^\mu$ ) and the redshift invariant observables ( $T_\infty, L_\infty$ ), so the resulting equations retain the familiar structure with explicit  $N(r)$  factors.

##### 4.1. Continuity equation

We begin with the continuity equation for the rest-mass (baryon) current:

$$\nabla_\mu (\rho u^\mu) = \frac{1}{\sqrt{-g}} \partial_\mu (\sqrt{-g} \rho u^\mu) = 0, \quad (34)$$

where  $\rho$  is the proper density,  $u^\mu$  the fluid four-velocity, and  $g$  the metric determinant.

Assuming stationarity ( $\partial_t = 0$ ), spherical symmetry, and purely radial motion  $u^\mu = (u^t, u^r, 0, 0)$ , continuity reduces to

$$\partial_r (r^2 \rho u^r) = 0 \implies r^2 \rho u^r = \text{const.} \quad (35)$$

This is the relativistic analogue of Equation 7; the invariance arises because  $\sqrt{-g} = r^2 \sin \theta$  in Schwarzschild. Inward flow has  $u^r < 0$  (since  $r$  increases outward). To keep the inward mass flux positive, we define

$$J \equiv -r^2 \rho u^r = \frac{\dot{M}}{4\pi} > 0, \quad (36)$$

which coincides with the non-relativistic definition used earlier (up to the sign choice).

##### 4.2. Radial Euler

The Euler equation follows from local energy-momentum conservation for a perfect fluid,

$$T^{\mu\nu} = (\varepsilon + P) u^\mu u^\nu + P g^{\mu\nu}, \quad (37)$$

with proper energy density  $\varepsilon$  and pressure  $P$ .

By contracting  $g_{r\mu} \nabla_\nu T^{\mu\nu} = 0$  (equivalently  $\nabla_\nu T_r^\nu = 0$ ) and using spherical symmetry, after some algebra we obtain the steady radial Euler equation

$$(\varepsilon + P) u^r \partial_r u_r = - (1 + u_r u^r) \partial_r P \quad (38)$$

$$- (\varepsilon + P) \frac{N'}{N} (1 + 2 u_r u^r).$$

In the regimes of interest, subsonic and low enthalpy regime<sup>6</sup>, the internal energy is small compared to the rest mass energy, ( $|u_r u^r| \ll 1, P \ll \varepsilon$ ). Then Equation 38 reduces to

$$\rho u^r \partial_r u_r = - \partial_r P - \frac{\rho c^2}{2} \partial_r \ln(N^2), \quad (39)$$

using  $\varepsilon \simeq \rho c^2$  at our working order (rest-mass dominated gas;  $P \ll \varepsilon$  and  $|u_r u^r| \ll 1$ ). Indeed, in the static limit  $u^r = 0$ , Equation 39 gives  $dP/dr = -(\rho c^2/2) d \ln(N^2)/dr = -(\rho c^2) N'/N$ , i.e. the test-fluid TOV balance in Schwarzschild. Furthermore, for weak fields and small speeds ( $N \rightarrow 1, u_r \simeq v^r$ ), the gravitational term becomes  $-(c^2/2) d \ln(N^2)/dr \simeq -GM/r^2 \equiv g$ , and Equation 39 reduces to the Newtonian form Equation 8.

##### 4.3. Radiative diffusion equation

In the Eckart frame (i.e., heat flux is orthogonal to the four velocity,  $q_\mu u^\mu = 0$ ), the total energy-momentum tensor is given by

$$T_{\mu\nu} = (\varepsilon + P) u_\mu u_\nu + P g_{\mu\nu} + u_\mu q_\nu + u_\nu q_\mu + \pi_{\mu\nu}, \quad (40)$$

where  $\varepsilon$  is the proper energy density (with  $\varepsilon \simeq \rho c^2$  in the rest-mass dominated regime used here),  $P$  is the isotropic gas pressure, and  $\pi_{\mu\nu}$  is the viscous stress tensor. In the slow settling limit  $|u^r| \ll 1$  we may neglect  $O(u^r)$  corrections in the diffusion closure and take  $u^\mu \simeq (N^{-1}, 0, 0, 0)$ . For spherical symmetry and stationarity configuration we have  $q^\mu = (0, q^r(r), 0, 0)$  and the viscous terms  $\pi_{\mu\nu}$  vanish by symmetry.

In the diffusion limit, (i.e., mean free path  $\lambda \ll$  gradient scale), the radiation mediated heat flux obeys (Misner et al. (1973)[Equation 22.16i])

$$q^\mu = -\kappa_T h^{\mu\nu} (\nabla_\nu T + T a_\nu), \quad (41)$$

where  $h^{\mu\nu} = g^{\mu\nu} + u^\mu u^\nu$ , and  $\kappa_T$  is Rosseland mean thermal conductivity

$$\kappa_T = \frac{16\sigma T^3}{3\kappa\rho}, \quad (42)$$

<sup>6</sup> Here  $\rho$  is the proper rest mass density used in the continuity equation. With  $\varepsilon \simeq \rho c^2$  the distinction between  $\varepsilon$  and  $\rho$  is immaterial at our working order; factors of  $c$  are kept explicitly in  $N(r)$ .

where  $\sigma$  is the Stefan–Boltzmann constant,  $\kappa$  is the opacity. And,  $a_\nu = u^\alpha \nabla_\alpha u_\nu$ , where in the static coordinates reduces to

$$a_r = \frac{1}{N} \frac{dN}{dr}, \quad a_t = a_\theta = a_\varphi = 0. \quad (43)$$

Because  $u^\mu$  has only a time component, we have  $h^{rr} = g^{rr} = N^2$ . Substituting into the heat flux expression [Equation 41](#) gives

$$\begin{aligned} q^r &= -\frac{16\sigma T^3}{3\kappa\rho} N^2 \left( \frac{dT}{dr} + T \frac{1}{N} \frac{dN}{dr} \right) \\ &= -\frac{16\sigma T^3}{3\kappa\rho} N \left( \frac{d}{dr}(NT) \right). \end{aligned} \quad (44)$$

Using the measured temperature at infinity  $T_\infty \equiv NT$ , leads to

$$q^r = -\frac{16\sigma T^3}{3\kappa\rho} N \frac{dT_\infty}{dr}. \quad (45)$$

In the other hand, in a stationary spacetime with time-like Killing vector  $K^\mu = (\partial/\partial t)^\mu$ , define the energy current

$$J^\mu \equiv T^{\mu\nu} K_\nu. \quad (46)$$

Because  $\nabla_\mu T^{\mu\nu} = 0$  and  $K^\mu$  is Killing,  $\nabla_\mu J^\mu = 0$ .

Let  $S_r$  be the 2-sphere of areal radius  $r$  and consider the timelike worldtube  $\mathcal{W}_r \equiv S_r \times [t, t+dt]$  with outward unit normal  $n_\mu = (0, N^{-1}, 0, 0)$  and induced 3-metric determinant  $\sqrt{-h} = Nr^2 \sin \theta$ . The proper 3-surface element on this world-tube is  $d\Sigma_\mu = n_\mu N dA dt$ , where  $dA = r^2 \sin \theta d\theta d\phi$  is the proper area element on  $S_r$ . The luminosity measured at infinity (Killing energy flux per unit Killing time) is therefore

$$L_\infty(r) \equiv -\frac{d}{dt} \int_{\mathcal{W}_r} J^\mu d\Sigma_\mu = - \int_{S_r} J^\mu n_\mu N dA, \quad (47)$$

and Gauss' theorem (using  $\nabla_\mu J^\mu = 0$ ) implies that  $L_\infty(r)$  is independent of  $r$  outside source regions.

Using our stress-energy decomposition [Equation 40](#) with  $u^\mu \simeq (N^{-1}, 0, 0, 0)$  and purely radial heat flux  $q^\mu = (0, q^r, 0, 0)$  satisfying  $u_\mu q^\mu = 0$ , we have  $u \cdot n = 0$ ,  $K \cdot n = 0$ , and  $q \cdot K = 0$ , and hence

$$J^\mu n_\mu = (u \cdot K) (q \cdot n) = (-N) (q^r N^{-1}) = -q^r. \quad (48)$$

Therefore

$$L_\infty(r) = \int_{S_r} N q^r dA = 4\pi r^2 N q^r. \quad (49)$$

If  $F_{\hat{r}}$  denotes the local (orthonormal) diffusive flux measured by local static (orthonormal) observers, then  $F_{\hat{r}} = q^r/N$ , so  $L_\infty = N^2 L_{\text{loc}}$  with  $L_{\text{loc}} = 4\pi r^2 F_{\hat{r}}$ .

Substituting [Equation 45](#) into [Equation 49](#) gives

$$L_\infty = -\frac{64\pi\sigma T^3}{3\kappa\rho} r^2 N^2 \frac{dT_\infty}{dr}. \quad (50)$$

Equivalently, eliminating  $q^r$  between [Equation 49](#) and [Equation 45](#) and solving for the gradient yields

$$\frac{dT_\infty}{dr} = -\frac{3\kappa\rho}{64\pi\sigma} \frac{N}{r^2 T_\infty^3} L_\infty. \quad (51)$$

Alternative classical derivation also matches also this result (see [Appendix D](#)). Moreover, in a static gravitational field thermal equilibrium implies the Tolman–Ehrenfest relation ([Tolman & Ehrenfest 1930](#); [Tolman 1934](#)). Furthermore, in the weak limit  $N \rightarrow 1$  (so that  $T_\infty \rightarrow T$  and  $L_\infty$  reduces to the standard radiative diffusion law, which is the Newtonian limit of the relativistic heat-flux relation ([Misner et al. \(1973\)](#)[Equation 22.16i]).

#### 4.4. Rationalized Form

It is convenient to absorb redshift factors into the dependent variables and non-dimentionalize with respect to base values  $N_f \equiv N(r_f)$ ,  $\rho_f$ , and  $T_{\text{eq}}$ :

$$\bar{x} = \frac{N^2 \rho}{N_f^2 \rho_f}, \quad (52a)$$

$$\bar{y} = \frac{NT}{T_{\text{eq}}} = \frac{T_\infty}{T_{\text{eq}}}, \quad (52b)$$

$$s = \frac{r - 2r_g}{h}, \quad (52c)$$

with  $r_g \equiv GM/c^2$  and the scale

$$h \equiv \frac{y_{\text{eq}}}{c^2} / \left. \frac{dN}{dr} \right|_f \approx \frac{kT_{\text{eq}}}{m|g|}, \quad |g| = \frac{GM}{N_f r_f^2}, \quad (53)$$

where

$$y_{\text{eq}} \equiv k T_{\text{eq}}/m. \quad (54)$$

For Schwarzschild,  $dN/dr = GM/(r^2 c^2 N)$ ; with  $r \simeq r_f$  this gives  $h \partial_r N \simeq (y_{\text{eq}}/c^2)(N_f/N)$ , hence this matches the NR form up to the extra redshift factor  $N_f$ . We use the conserved mass flux defined in [Equation 36](#), so that

$$u_r = \frac{u^r}{N^2} = -\frac{J}{r^2 \rho_f N_f^2 \bar{x}}. \quad (55)$$

The (Killing-energy) luminosity is conserved through the layers, i.e.,  $L_\infty = \text{const}$ . Using Equations (35), (39), and (51) with  $P = \rho kT/m$ , and using  $\partial_s = h \partial_r$  together with Equations (52)–(55), after replacing  $u^r$  and normalizing by  $y_{\text{eq}}$  one obtains

$$\partial_s \bar{x} = \bar{x} \frac{-\frac{N_f}{N} + \underbrace{\frac{3\bar{y}y_{\text{eq}}}{c^2} \frac{N_f}{N^2}}_{\text{hydrostatic}} + \underbrace{\frac{3\tau_h N_f^2}{16} \frac{L_\infty}{L_{\text{eq}}} \frac{1}{N} \frac{\bar{x}}{\bar{y}^3}}_{\text{diffusion}}}{\bar{y} - \left( \frac{N}{N_f} \right)^3 \mathcal{T}^2 \frac{\bar{y}_f}{\bar{x}^2}}. \quad (56)$$

where  $\tau_h$  is given by [Equation 31](#), and

$$L_{\text{eq}} \equiv \eta \dot{M} c^2 \equiv \frac{4\pi r_s^2}{N_s^2} \sigma T_{\text{eq}}^4, \quad N_s \equiv N(r_s). \quad (57)$$

Here, the  $1/N$  in the diffusion term is the redshift correction in the relativistic diffusion law, and the factor  $N_f^2$  arises because the density variable carried by  $\bar{x}$  is the  $N^2 \rho$  at the base. In a static Schwarzschild atmosphere the proper radial distance is  $dl = dr/N$ , so the true optical depth across a thickness  $\Delta r \sim h$  is

$$\tau_{\text{true,h}} = \int_{r_f}^{r_f+h} \kappa \rho dl \simeq \kappa \rho_f \int_{r_f}^{r_f+h} \frac{dr}{N} \simeq \frac{\kappa \rho_f h}{N_f}, \quad (58)$$

where we used the thin-layer approximation ( $\rho \simeq \rho_f$ ,  $N \simeq N_f$ ). Thus  $\tau_h$  differs from  $\tau_{\text{true,h}}$  only by the known factor  $N_f$ ; it is a convenient way of carrying the base optical depth through the algebra.

At the foil ( $r = r_f$ ) we impose the kinetic boundary condition

$$J = \frac{\dot{M}}{4\pi} = N_f r_f^2 \mathcal{T} \rho_f \sqrt{\frac{kT_f}{m}}, \quad (59)$$

with  $\rho_f \equiv \rho(r_f)$  and  $T_f \equiv T(r_f)$ . This is the only place where  $\mathcal{T}$  enters; it is the kinetic boundary (mass flux per unit proper area times proper thermal speed) and enforces  $|\mathcal{T}| < 1$ . Since, using barred variables

$$\rho(r) = \frac{N_f^2 \rho_f}{N(r)^2} \bar{x}(r), \quad T(r) = \frac{T_{\text{eq}}}{N(r)} \bar{y}(r), \quad (60)$$

and  $y_{\text{eq}}$  is given by [Equation 54](#), we note

$$\sqrt{\frac{kT_f}{m}} = \sqrt{\frac{y_{\text{eq}} \bar{y}_f}{N_f}}, \quad \bar{y}_f \equiv \bar{y}(r_f) = \frac{N_f T_f}{T_{\text{eq}}}. \quad (61)$$

Hence

$$J = r_f^2 \mathcal{T} \rho_f N_f^{1/2} \sqrt{y_{\text{eq}} \bar{y}_f}. \quad (62)$$

Therefore, the relativistic sonic term, relativistic analogue of [Equation 13](#), that appears in the denominator of  $\partial_s \bar{x}$  in [Equation 56](#) can be written;

$$D(r) \equiv \frac{\underbrace{y_{\text{eq}} \bar{y}}_{NkT/m} - \underbrace{\frac{J^2}{r^4} \frac{1}{N \rho^2}}_{\text{inertial term}}}{.} \quad (63)$$

Eliminating  $J$  with [Equation 62](#) and evaluating at the base ( $r = r_f$ ,  $N = N_f$ ,  $\bar{x}_f = 1$ ,  $\bar{y} = \bar{y}_f$ ) gives

$$D_f \equiv D(r_f) = y_{\text{eq}} \bar{y}_f (1 - \mathcal{T}^2). \quad (64)$$

Dividing by  $y_{\text{eq}}$  the common positive factor (as is done when one rationalizes the ODE) gives the dimensionless base discriminant  $\bar{y}_f(1 - \mathcal{T}^2)$ , hence the subsonic base condition is precisely

$$\bar{y}_f(1 - \mathcal{T}^2) > 0 \Leftrightarrow |\mathcal{T}| < 1. \quad (65)$$

In addition, the barred diffusion equation has the form

$$\partial_s \bar{y} = - \frac{3 \tau_h N_f^2}{16} \frac{L_\infty}{L_{\text{eq}}} \frac{1}{N} \frac{\bar{x}}{\bar{y}^3}, \quad (66)$$

so for accretion powered configurations ( $L_\infty \leq 0$ ),  $\partial_s \bar{y} > 0$  and  $T_\infty$  rises outward, this implies convective stability for the layer.

Further, at the boundary  $r = r_f$  fixes  $\rho_f$  (or  $J$ ), and we have

$$\bar{x}_f = 1, \quad (67a)$$

$$\bar{y}_f = \frac{N_f T_f}{T_{\text{eq}}}. \quad (67b)$$

At the top of the layer ( $r = r_s$ ), the luminosity balance with the accretion flow

$$L_\infty = \frac{4\pi r_s^2}{N_s^2} \sigma T_{\infty,s}^4 - L_{\text{eq}} = L_{\text{eq}} (\bar{y}_s^4 - 1), \quad (68)$$

where  $T_{\infty,s} = N_s T_s$ . Normal stress balance across the interface gives the ram pressure match. On the atmospheric side the normal stress is just the gas pressure,

$$P_s = \rho_s \frac{kT_s}{m}. \quad (69)$$

Using the barred definitions [Equation 60](#) one finds

$$P_s = \frac{N_f^2 \rho_f y_{\text{eq}}}{N_s^3} \bar{x}_s \bar{y}_s. \quad (70)$$

On the accretion side, for a cold, hypersonic upstream the normal momentum flux is

$$T^r_r \simeq \frac{\rho_a (u_a^r)^2}{N_s^2}. \quad (71)$$

Using spherical steady continuity at the shock,

$$\dot{M} = -4\pi r_s^2 \rho_a u_a^r \Rightarrow \rho_a = \frac{\dot{M}}{4\pi r_s^2 |u_a^r|}, \quad (72)$$

gives

$$T^r_r \simeq \frac{\dot{M} u_a^r}{4\pi r_s^2 N_s^2}. \quad (73)$$

In a purely ballistic free fall one would take  $u_a^r$  at its relativistic value and recover the standard matching. In practice, a fraction of the available binding energy can be radiated away or turned into a wind; the same processes reduce the residual impact speed and hence the incident momentum flux. So by parametrizing the residual impact speed by an impact efficiency  $0 < \eta_{\text{ram}} \leq 1$  via  $|u_a^r| \equiv \eta_{\text{ram}} c$ , [Equation 73](#) becomes

$$T^r_r \simeq \eta_{\text{ram}} \frac{\dot{M} c}{4\pi r_s^2 N_s^2}, \quad (74)$$

Equating the normal stresses across the thin interface,  $P_s \simeq T^r r$ , and substituting [Equation 70](#)-[Equation 74](#) yields the jump condition

$$\bar{x}_s \bar{y}_s \simeq \eta_{\text{ram}} \frac{\dot{M} c}{4\pi r_s^2} \frac{N_s}{N_f^2 \rho_f y_{\text{eq}}}. \quad (75)$$

To eliminate  $\rho_f$  we use the kinetic boundary condition at the foil [Equation 59](#) which implies

$$\rho_f = \frac{\dot{M}}{4\pi} \frac{1}{N_f r_f^2 \mathcal{T}} \sqrt{\frac{m}{kT_f}} = \frac{\dot{M}}{4\pi} \frac{1}{r_f^2 \mathcal{T}} \frac{1}{N_f^{1/2} \sqrt{y_{\text{eq}} \bar{y}_f}}. \quad (76)$$

Insert this into [Equation 75](#) and simplify; using  $|g| h = y_{\text{eq}}$  (from  $|g| = GM/(N_f r_f^2)$  and  $h = y_{\text{eq}} N_f r_f^2 / (GM)$ ) one obtains

$$\bar{x}_s \bar{y}_s \simeq \eta_{\text{ram}} \frac{\mathcal{T} c}{\sqrt{|g| h}} \left( \frac{r_f}{r_s} \right)^2 \frac{N_s}{N_f^{3/2}} \bar{y}_f^{1/2}. \quad (77)$$

In the thin-layer limit  $r_s \simeq r_f$ , this reduces to  $\bar{x}_s \bar{y}_s \simeq \eta_{\text{ram}} (\mathcal{T} c / \sqrt{|g| h}) (N_s / N_f^{3/2}) \bar{y}_f^{1/2}$ . In our baseline set-up the upstream just above the atmosphere is a cold, relativistic infall with negligible mass loading and quasi-isotropic radiative losses. In the local static frame at  $r_s$ , the radial momentum flux and (Killing-energy) flux differ by a factor  $c$  for a cold stream; hence any process that removes a fixed fraction of the available energy reduces the radial momentum flux by the same fraction. Under these conditions one may identify  $\eta_{\text{ram}} = \eta$  (the efficiency appearing in  $L_{\text{eq}} = \eta \dot{M} c^2$ ). If mass loading or anisotropic momentum loss is significant upstream, keep  $\eta_{\text{ram}}$  distinct; all subsequent formulae remain valid with the replacement  $\eta \rightarrow \eta_{\text{ram}}$ .

In addition, with  $L_\infty \leq 0$  and  $kT \ll mc^2$  the relativistic enthalpy correction appears in the numerator of  $\partial_s \bar{x}$ , is small. At the base its ratio to the hydrostatic term is

$$\left. \frac{\text{enthalpy}}{\text{hydrostatic}} \right|_{r_f} = 3 \frac{kT_f}{mc^2}, \quad (78)$$

so, it becomes comparable to hydrostatic only if  $kT_f \sim mc^2/3$ , independent of  $N_f$ . Expressed in terms of the redshifted temperature, this is  $N_f \lesssim 3 kT_{\infty,f} / mc^2$ , but the controlling quantity is  $T_f$ . For baryons this would require  $T_f \gtrsim 3 \times 10^{12}$  K (protons), far above the temperatures of interest, so the enthalpy term is negligible here.

#### 4.5. Approximate Solution

In the limit  $r_f \gg r_g$ , one has  $N \simeq 1$  for all  $r \geq r_f$  and, for  $y_{\text{eq}} \ll c^2$ , [Equation 56](#) reduces to the nonrelativistic system [Equation 32](#); the solutions are then similar. We therefore confine attention to the compact surface limit,  $s h \ll r_g$ , and assume  $|L_\infty|$  is small so that a scale separation between  $\bar{x}$  and  $\bar{y}$  exists (i.e.  $\bar{y}$  varies weakly across the layer).

For  $s \equiv (r - 2r_g)/h \ll r_g/h$ , we obtain

$$N(r) \simeq \sqrt{\frac{sh}{2r_g}}, \quad \frac{N}{N_f} \simeq \sqrt{\frac{s}{s_f}}, \quad (79)$$

with  $s_f \equiv (r_f - 2r_g)/h$  and  $N_f = N(r_f)$ . Using  $h \equiv (y_{\text{eq}}/c^2)/(\partial_r N)_f$  and  $(\partial_r N)_f = r_g/(N_f r_f^2)$ , one finds

$$\begin{aligned} N_f^2 &\approx \frac{s_f h}{2r_g} = \frac{s_f}{2r_g} \frac{y_{\text{eq}}}{c^2} \frac{N_f r_f^2}{r_g} \\ &\Rightarrow N_f \approx s_f \frac{y_{\text{eq}}}{c^2} \frac{r_f^2}{2r_g^2}. \end{aligned} \quad (80)$$

In the near-horizon limit  $r_f \simeq 2r_g$  this reduces to

$$N_f \approx 2s_f \frac{kT_{\text{eq}}}{mc^2}, \quad (81)$$

And, correspondingly,

$$h = \frac{y_{\text{eq}}}{c^2} \frac{N_f r_f^2}{r_g} \approx 4N_f \frac{kT_{\text{eq}}}{mc^2} r_g = 8s_f \left( \frac{kT_{\text{eq}}}{mc^2} \right)^2 r_g, \quad (82)$$

so the scale height decreases linearly with  $s_f$  (more compact surfaces  $\Rightarrow$  smaller  $h$ ).

We consider two regimes:

*Regime A: enthalpy correction negligible* ( $kT_f \ll mc^2$ , so the positive pressure/enthalpy term in [Equation 56](#) can be dropped). With  $|L_\infty|$  small, take  $\bar{y} \simeq \tilde{y}$  constant across the layer as a characteristic rationalized temperature and neglect the diffusion term in the  $\partial_s \bar{x}$  equation. Then the hydrostatic piece of [Equation 56](#) gives

$$\partial_s \bar{x} \simeq -\frac{\bar{x}}{\tilde{y}} \frac{N_f}{N} = -\frac{\bar{x}}{\tilde{y}} \sqrt{\frac{s_f}{s}}. \quad (83)$$

Integration yields

$$\begin{aligned} \bar{x}(s) &\simeq \exp \left[ -\frac{2}{\tilde{y}} \left( \sqrt{s_f s} - s_f \right) \right] \\ &= \rho_f \frac{N_f^2}{N^2} \bar{x} = \rho_f \frac{s_f}{s} \exp \left[ -\frac{2s_f}{\tilde{y}} \left( \sqrt{\frac{s}{s_f}} - 1 \right) \right]. \end{aligned} \quad (84)$$

Thus, the density (sub)exponentially decreases. As comparing with NR case [Equation 28a](#) in the NR atmosphere (small redshift,  $r_f \gg r_g$  gravity is essentially constant over a scale height [Equation 4](#)). We have defined

$$s_{\text{NR}} = \frac{r - r_f}{H}. \quad (85)$$

The hydrostatic equation in that limit becomes (with almost constant  $T$ )

$$\frac{d\rho}{dr} \simeq -\frac{\rho}{H}, \quad \Rightarrow \quad \frac{d \ln \rho}{ds_{\text{NR}}} \simeq -1, \quad (86)$$

so

$$\bar{x}_{\text{SN}}(s_{\text{NR}}) = \frac{\rho}{\rho_f} \simeq \exp[-s_{\text{NR}}]. \quad (87)$$

In GR part we defined  $s = (r - 2r_g)/h$  and then used the near-horizon relation  $N \sim \sqrt{s}$  to pull all redshift dependence into  $s$ , so the same symbol  $s$  is not the same "linear height" as in the NR section; it is matched to the GR geometry. Thus, in NR, the local hydrostatic balance sees a constant gravitational acceleration, so  $\rho$  decays like an ordinary exponential with height. In the near-horizon GR limit, the gravitational redshift factor  $N$  changes as  $\sqrt{r - 2r_g}$  and we see that directly in the  $\sqrt{s}$  that appears in the exponent.

Expanding  $\sqrt{s/s_f} = 1 + (s - s_f)/(2s_f)$ , the local e-folding thickness in  $s$  is

$$\Delta s_{\text{efold}} = \left( \frac{1}{s_f} + \frac{1}{\tilde{y}} \right)^{-1} \simeq \tilde{y}, \quad (s_f \gg \tilde{y}), \quad (88)$$

near the base, so the physical thickness is

$$\Delta r \simeq h \Delta s_{\text{efold}} \propto s_f. \quad (89)$$

Hence, more compact surfaces (smaller  $s_f$ ) have a thinner atmosphere, consistent with what we had earlier that  $h$  decreasing linearly with  $s_f$ .

The associated temperature profile follows from the relativistic diffusion equation in Equation 56. With  $\bar{x} \simeq \tilde{x}$  and  $N^{-1} \simeq \sqrt{2r_g}/(s h)$ ,

$$\begin{aligned} \partial_s \bar{y} &\simeq - \frac{3 \tau_h N_f^2}{16} \frac{L_\infty}{L_{\text{eq}}} \frac{1}{N} \frac{\tilde{x}}{\bar{y}^3} \\ &= - \frac{3 \tau_h N_f^2}{16} \frac{L_\infty}{L_{\text{eq}}} \sqrt{\frac{2r_g}{s h}} \frac{\tilde{x}}{\bar{y}^3}. \end{aligned} \quad (90)$$

Thus

$$\bar{y}(s) = \left[ \bar{y}_f^4 - \frac{3}{2} \bar{\tau} N_f^2 \frac{L_\infty}{L_{\text{eq}}} \sqrt{\frac{2r_g}{h}} (\sqrt{s} - \sqrt{s_f}) \right]^{1/4}, \quad (91)$$

where  $\bar{\tau} \equiv \tau_h \tilde{x}$  and  $\tau_h$  is given by Equation 31.

*Surface luminosity.* Using  $L_\infty = L_{\text{eq}}(\bar{y}_s^4 - 1)$ , and the integrated profile for  $\bar{y}^4$ , we obtain

$$\begin{aligned} L_{\text{surf}} &\equiv L_{\text{eq}} \bar{y}_s^4 \\ &= \frac{L_{\text{eq}} \bar{y}_f^4 + \frac{3}{2} \bar{\tau} N_f^2 L_{\text{eq}} \sqrt{\frac{2r_g}{h}} (\sqrt{s_s} - \sqrt{s_f})}{1 + \frac{3}{2} \bar{\tau} N_f^2 \sqrt{\frac{2r_g}{h}} (\sqrt{s_s} - \sqrt{s_f})}. \end{aligned} \quad (92)$$

Since  $\bar{y}_f = T_{\infty,f}/T_{\text{eq}} = N_f T_f/T_{\text{eq}}$  and  $r_s \simeq r_f$ , the base term is

$$\begin{aligned} L_{\text{eq}} \bar{y}_f^4 &= \frac{4\pi r_f^2}{N_f^2} \sigma T_{\infty,f}^4 \\ &= 4\pi r_f^2 \sigma N_f^2 T_f^4 \equiv L_{\text{foil},\infty}. \end{aligned} \quad (93)$$

Equivalently, if one prefers the local definition  $L_{\text{foil}} = 4\pi r_f^2 \sigma T_f^4$ , then  $L_{\text{eq}} \bar{y}_f^4 = N_f^2 L_{\text{foil}}$ . In either form,

$$L_{\text{surf}} = \frac{L_{\text{foil},\infty} + \frac{3}{2} \bar{\tau} N_f^2 L_{\text{eq}} \sqrt{\frac{2r_g}{h}} (\sqrt{s_s} - \sqrt{s_f})}{1 + \frac{3}{2} \bar{\tau} N_f^2 \sqrt{\frac{2r_g}{h}} (\sqrt{s_s} - \sqrt{s_f})}. \quad (94)$$

Thus, even for very compact surfaces one obtains  $L_{\text{surf}} \rightarrow L_{\text{eq}} = \eta \dot{M} c^2$  i.e., it radiates at the equilibrium rate. To make it clear let us compare it to NR case. Here the role of  $(3/4)\bar{\tau}$  in Equation 23 is played by the whole combination

$$A \equiv \frac{3}{2} \bar{\tau} N_f^2 \sqrt{\frac{2r_g}{h}} (\sqrt{s} - \sqrt{s_f}), \quad (95)$$

Then our GR expression is just

$$L_{\text{surf}} = \frac{L_{\text{foil}} + A L_{\text{eq}}}{1 + A}. \quad (96)$$

So to keep this similarity, we define dimensionless combination

$$\bar{\tau}_{\text{GR}} \equiv 2 \bar{\tau} N_f^2 \sqrt{\frac{2r_g}{h}} (\sqrt{s} - \sqrt{s_f}), \quad (97)$$

the 2 is the only new geometric factor from integrating  $1/N \propto s^{-1/2}$  in the near-horizon geometry, and the extra  $4/3$  is just a choice of normalization so that the GR and NR  $L_{\text{surf}}$  formulas Equation 23 look identical. Thus, we obtain

$$L_{\text{surf}} = \frac{L_{\text{foil},\infty} + \frac{3}{4} \bar{\tau}_{\text{GR}} L_{\text{eq}}}{1 + \frac{3}{4} \bar{\tau}_{\text{GR}}}, \quad (98)$$

and the optically thick condition is just

$$\frac{3}{4} \bar{\tau}_{\text{GR}} \gg 1. \quad (99)$$

It is worth mentioning that, despite its algebraic complexity,  $\bar{\tau}_{\text{GR}}$  is nothing more than the usual comoving optical depth of the settling layer. Therefore,  $\bar{\tau}_{\text{GR}}$  indeed is the GR optical depth written in our rescaled variables, and the condition  $\bar{\tau}_{\text{GR}} \gg 1$  is exactly the usual requirement that the layer be optically thick between the foil and the photosphere.

*Regime B: enthalpy correction important* (rare in practice). The positive pressure/enthalpy term in the numerator of Equation 56 competes with the hydrostatic term when  $3 \frac{kT_f}{mc^2} \sim 1$ . This criterion is independent of  $N_f$ ; it requires ultra-relativistic baryon temperatures and is not met for the sources of interest.

Formally keeping this term and still neglecting diffusion (small  $|L_\infty|$ ), and taking the subsonic-base limit so the denominator is  $\simeq \bar{y} \simeq \tilde{y}$ , we obtain

$$\partial_s \bar{x} \simeq \bar{x} \left[ \frac{3 y_{\text{eq}}}{c^2} \frac{N_f}{N^2} - \frac{1}{\tilde{y}} \frac{N_f}{N} \right]. \quad (100)$$

Using  $N_f/N = \sqrt{s_f/s}$  and, in the near-horizon limit,

$$\frac{N_f}{N^2} = \frac{2r_g N_f}{h} \frac{1}{s} = \frac{c^2}{2y_{\text{eq}}} \frac{1}{s}, \quad (101)$$

this reduces to

$$\partial_s \ln \bar{x} \simeq \frac{3}{2} \frac{1}{s} - \frac{1}{\tilde{y}} \sqrt{\frac{s_f}{s}}. \quad (102)$$

Integrating gives

$$\bar{x}(s) \simeq \left(\frac{s}{s_f}\right)^{3/2} \exp\left[-\frac{2\sqrt{s_f}}{\tilde{y}}(\sqrt{s} - \sqrt{s_f})\right]. \quad (103)$$

When the enthalpy term dominates near the base (i.e.  $3kT_f/mc^2 > 1$ ),  $\bar{x}$  (and thus  $\rho$ ) initially increases with radius; the pressure nevertheless decreases outward because  $P \propto \bar{x}/N^3$  and  $N \propto \sqrt{s}$  near the horizon, so the  $s^{3/2}$  rise is canceled by the geometric  $N^{-3}$  factor, leaving the hydrostatic exponential to enforce  $dP/dr < 0$ . The density peaks where  $d\ln \bar{x}/ds = 0$ , which gives

$$s_{\text{peak}} = \frac{9}{4} \frac{\tilde{y}^2}{s_f}. \quad (104)$$

Therefore, at the peak (and in the compact limit  $s_{\text{peak}} \gg s_f$ ) we obtain

$$\bar{x}_{\text{peak}} \simeq \left(\frac{s_{\text{peak}}}{s_f}\right)^{3/2} \exp(-3) = \frac{27}{8} \frac{\tilde{y}^3}{s_f^3} e^{-3}. \quad (105)$$

Setting  $\tilde{x} = \bar{x}_{\text{peak}}$ , the temperature is approximately given by Equation 91 (with the corrected coefficient in that equation), with the attendant consequences for  $L_{\text{surf}}$ .

Physically, in Regime B the gas is relativistically hot, i.e., the relativistic enthalpy and inertia terms are comparable those associated with gravity. Nevertheless, the local temperature  $T = T_{\infty}/N$  drops outward as  $N$  rises, and does so sufficiently fast that  $P = \rho kT/m$  decreases even if  $\rho$  increases with radius initially before ultimately falling.

## 5. BOUNDARY CONDITION CONSIDERATIONS

There are a number of constraints on the parameters imposed by the boundary conditions. We review these here in terms of convenient parametrizations of the foil surface properties. We note that we assume locality, i.e., that the foil surface can only interact with matter that impinges upon it.

### 5.1. Mass Flow

Already, we have explicitly noted the need for

$$\mathcal{T}^2 < 1, \quad (106)$$

limiting the rate at which the foil can absorb accreting baryonic matter. (Black holes explicitly violate this condition.) This implicitly imposes conditions on the surface redshift.

Because the pressure is monotonically decreasing with radius in our solutions, the pressure at the base must be at least the post shock pressure:

$$P_f = \frac{\dot{M} y_{\text{eq}}^{1/2}}{4\pi r_f^2 \mathcal{T}} \frac{\tilde{y}_f^{1/2}}{N_f^{3/2}} \geq \frac{\eta \dot{M} c}{4\pi r_s^2 N_s^2}, \quad (107)$$

This gives a lower bound on  $\bar{y}_f$  and hence on  $T_f (= \bar{y}_f T_{\text{eq}}/N_f)$ :

$$\begin{aligned} \bar{y}_f &\geq \eta_{\text{ram}}^2 \mathcal{T}^2 \left(\frac{r_f}{r_s}\right)^4 \frac{N_f^3}{N_s^4} \frac{mc^2}{kT_{\text{eq}}} \\ \iff T_f &\geq \eta_{\text{ram}}^2 \mathcal{T}^2 \left(\frac{r_f}{r_s}\right)^4 \frac{N_f^2}{N_s^4} \frac{mc^2}{k}. \end{aligned} \quad (108)$$

As  $\mathcal{T} \rightarrow 0$ , this bound allows  $T_f \rightarrow 0$ . Additionally, the atmosphere must be optically thick over a local scale height (as assumed by the diffusion closure), i.e.  $\tau > 1$ . For electron scattering,

$$\tau \approx \kappa \rho \frac{kT}{m|g|} = \frac{\kappa P}{|g|}, \quad (109)$$

so (since  $P$  decreases outward)  $\tau \lesssim \kappa P_f/|g|$ , and we must have

$$P_f = \frac{\dot{M} y_{\text{eq}}^{1/2}}{4\pi r_f^2 \mathcal{T}} \frac{\tilde{y}_f^{1/2}}{N_f^{3/2}} > \frac{|g|}{\kappa}. \quad (110)$$

Solving for  $T_f$  gives

$$T_f > \frac{m}{k} \mathcal{T}^2 \left(\frac{4\pi |g| r_f^2}{\kappa \dot{M}}\right)^2 N_f^2. \quad (111)$$

Using the height scale definition Equation 29 (which implies  $|g|r_f^2 = GM/N_f$ ), the explicit  $N_f$  cancels and we obtain

$$T_f > \frac{m}{k} \mathcal{T}^2 \left(\frac{4\pi GM}{\kappa \dot{M}}\right)^2. \quad (112)$$

Equivalently, in terms of  $L_{\text{eq}}$  and the Eddington luminosity  $L_{\text{Edd}} = 4\pi GMc/\kappa$ ,

$$T_f > \frac{mc^2}{k} \mathcal{T}^2 \eta^2 \left(\frac{L_{\text{Edd}}}{L_{\text{eq}}}\right)^2, \quad (113)$$

where we used  $L_{\text{eq}} = \eta \dot{M} c^2$ .

Which bound on  $T_f$  is more restrictive depends on  $\dot{M}$  (or  $L_{\text{eq}}$ ). The shock support bound scales as  $T_f \propto N_f^2$ , whereas the optical depth bound is independent of  $N_f$ . Thus the shock bound dominates only when

$$\left(\frac{r_f}{r_s}\right)^2 \frac{N_f}{N_s^2} > \frac{L_{\text{Edd}}}{L_{\text{eq}}}, \quad (114)$$

which, for typical Radiatively inefficient accretion flows (RIAFs) conditions  $L_{\text{eq}} \ll L_{\text{Edd}}$ , would require extremely large surface redshifts (often unattainable).

Finally, the emitting layer redshift is limited by the requirement that the solution extends beyond the density peak  $s_{\text{peak}}$ . Using the near horizon relation  $N^2 \simeq sh/(2r_g)$  and the Regime B peak Equation 104,

$$\begin{aligned} N_s^2 &= \frac{h s_s}{2r_g} > \frac{h s_{\text{peak}}}{2r_g} \\ &= 4 s_{\text{peak}} s_f \left(\frac{kT_{\text{eq}}}{mc^2}\right)^2 = 9 \tilde{y}^2 \left(\frac{kT_{\text{eq}}}{mc^2}\right)^2. \end{aligned} \quad (115)$$

Hence

$$N_s \gtrsim 3 \tilde{y} \frac{kT_{\text{eq}}}{mc^2}. \quad (116)$$

For  $kT_{\text{eq}}/(mc^2) \ll 1$  (e.g.  $T_{\text{eq}} \sim 10^4$  K for baryons), this lower bound on  $N_s$  is tiny, i.e. it is a very weak constraint on the photosphere redshift.

### 5.2. Energy Flow

Up to now we treated the gas temperature at the base of the atmosphere,  $T_f \equiv T(r_f)$ , as a free inner datum. However, local gas-surface microphysics constrains both  $T_f$  and the base temperature gradient  $\partial_r T|_f$ : even if the foil itself is extremely cold, baryon-baryon collisions and radiative diffusion generally prevent the base gas from cooling arbitrarily, producing an effective floor temperature. We model two local ingredients.

(i) *Energy accommodation in gas-surface collisions*.—Let  $T_{\bullet}$  denote the foil material temperature. A standard way to parametrize partial thermalization at the wall is with an energy-accommodation coefficient  $\epsilon \in [0, 1]$  defined by

$$T_{\text{refl}} = T_f + \epsilon(T_{\bullet} - T_f), \quad \epsilon \in [0, 1], \quad (117)$$

where  $T_{\text{refl}}$  is the effective temperature of particles immediately after reflection/interaction with the surface. For a simple elastic 1D collision model between a gas particle of mass  $m$  and a surface site of effective mass  $M$  (thermalized at  $T_{\bullet}$ ), one finds

$$\epsilon = \frac{4mM}{(m+M)^2}, \quad (118)$$

so  $\epsilon \rightarrow 0$  corresponds to nearly specular reflection ( $M \rightarrow \infty$ ) and  $\epsilon = 1$  corresponds to complete thermal accommodation ( $m = M$ ).

(ii) *Heat-flux balance at the wall*.—The net energy flux transferred from the foil to the gas (positive when energy flows from foil to gas) can be estimated kinetically as the particle flux incident on the wall times the energy gained per particle:

$$\begin{aligned} q_{\text{wall}} &\simeq \frac{1}{4} n c_v v_{\text{th}} (T_{\text{refl}} - T_f) \\ &= \frac{1}{4} n c_v \epsilon v_{\text{th}} (T_{\bullet} - T_f), \end{aligned} \quad (119)$$

where  $c_v = \frac{3}{2}k$ ,  $n$  is the baryon number density and  $v_{\text{th}}$  is a characteristic thermal speed. Within the gas, the collisional conductive flux is

$$q = -\kappa_c \partial_r T, \quad \kappa_c = \frac{1}{3} n c_v v_{\text{th}} \lambda_c, \quad (120)$$

with  $\lambda_c$  the baryon-baryon collisional mean free path near the wall. Matching  $q_{\text{wall}} = q$  at  $r = r_f$  eliminates

$n, c_v, v_{\text{th}}$  and yields a kinetic boundary condition on the base temperature gradient:

$$\partial_r T|_f = -\frac{3\epsilon}{4\lambda_c} (T_{\bullet} - T_f). \quad (121)$$

On the macroscopic side, the base temperature gradient is also set by radiative diffusion in the optically thick atmosphere. Using the same diffusion law as in the main text (evaluated locally over a microscopic distance  $\sim \lambda_c$ , across which  $N(r)$  is constant to excellent approximation),

$$\partial_r T|_f = -\frac{3\kappa\rho}{64\pi\sigma} \frac{L}{r_f^2 T_f^3} = -\frac{3}{64\pi\sigma} \frac{L}{r_f^2 \lambda T_f^3}, \quad (122)$$

where  $\lambda \equiv (\kappa\rho)^{-1}$  is the photon mean free path and  $L$  is the (radially conserved) luminosity (outward positive). Equating Equation 121 and Equation 122 gives an implicit local relation for  $T_f$ :

$$T_f^3 (T_f - T_{\bullet}) = \frac{T_{\text{eq}}^4}{4\epsilon} \frac{\lambda_c}{\lambda} \frac{|L|}{L_{\text{eq}}}, \quad (123)$$

where  $L_{\text{eq}} \equiv 4\pi r_f^2 \sigma T_{\text{eq}}^4$ . (The absolute value is convenient because in accretion-powered configurations the net luminosity through the layer is typically inward,  $L \leq 0$ .)

It is convenient to define the microphysical floor temperature

$$T_L \equiv T_{\text{eq}} \left( \frac{1}{4\epsilon} \frac{\lambda_c}{\lambda} \frac{|L|}{L_{\text{eq}}} \right)^{1/4}, \quad (124)$$

so that Equation 123 becomes

$$\left( \frac{T_f}{T_L} \right)^3 \left( \frac{T_f}{T_L} - \frac{T_{\bullet}}{T_L} \right) = 1. \quad (125)$$

Defining  $t_f \equiv T_f/T_L$  and  $s_{\bullet} \equiv T_{\bullet}/T_L$ , Equation 125 has a unique positive root with limits

$$s_{\bullet} \ll 1 : t_f = 1 + \frac{s_{\bullet}}{4} + O(s_{\bullet}^2) \Rightarrow T_f \simeq T_L, \quad (126)$$

$$s_{\bullet} \gg 1 : t_f = s_{\bullet} + \frac{1}{s_{\bullet}^3} + O(s_{\bullet}^{-7}) \Rightarrow T_f \simeq T_{\bullet} + \frac{T_L^4}{T_{\bullet}^3},$$

so  $T_f$  approaches  $T_{\bullet}$  from above for hot foils, while for cold foils ( $T_{\bullet} \rightarrow 0$ ) the base gas temperature cannot drop below  $T_L$ .

Because  $N(r)$  varies negligibly across the microscopic thickness  $\Delta r \sim \lambda_c$ , the same boundary condition applies in the relativistic treatment when expressed in redshift-invariant variables: replacing  $(T, L, T_{\text{eq}}, L_{\text{eq}})$  by  $(T_{\infty}, L_{\infty}, T_{\text{eq},\infty}, L_{\text{eq},\infty})$  multiplies both sides of Equation 123 by the same factor and leaves the relation unchanged up to  $\mathcal{O}(\lambda_c/\ell_g) \ll 1$ , with  $\ell_g \equiv N/|dN/dr|$ .

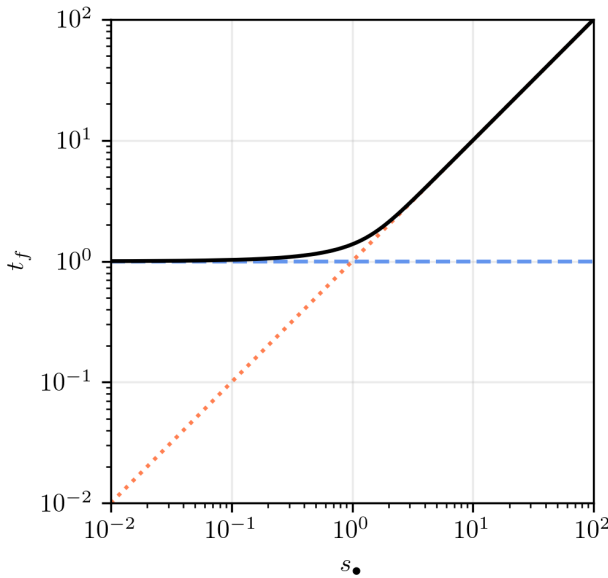


**Figure 2.** Microphysical floor on the base temperature from Equation 125 on log-log axes. Blue curve shows the solution of  $t^3(t - s_•) = 1$  with  $t_f \equiv T_f/T_L$  and  $s_• \equiv T_•/T_L$ . Black dashed line shows  $t_f = 1$  ( $T_f = T_L$ ). Red dotted line shows  $t_f = s_•$  ( $T_f = T_•$ ). For  $s_• \gg 1$  (hot foil),  $t_f \rightarrow s_•$  with a small upward offset  $T_L^4/T_•^3$ . Thus  $T_L$  sets a hard lower bound for the gas temperature at the base; it depends on  $\epsilon$ ,  $\lambda_c/\lambda$ , and the normalized luminosity  $|L|/L_{\text{eq}}$  via Equation 124.

## 6. SUMMARY AND CONCLUSIONS

We have constructed a minimal model of a steady, spherically symmetric, subsonic baryonic settling layer between an outer photosphere (or accretion shock) and a horizonless compact surface (a “foil”) embedded in an exterior Schwarzschild spacetime. The layer is gas-pressure supported and transports energy by radiative diffusion in the optically thick limit. We use the non-relativistic equations to build intuition and then formulate the full problem relativistically in terms of redshift-invariant observables.

The unknown surface physics is encoded through local boundary conditions at the foil. In particular, we parametrize the rate at which baryons are processed by the surface with a dimensionless transmittance parameter  $\mathcal{T}$  and allow the foil temperature to differ from the gas temperature. Subsonic settling restricts  $\mathcal{T}$  to be below unity in magnitude. At the outer interface we impose (i) energy balance with the accretion flow (setting the conserved luminosity at infinity) and (ii) normal-stress balance with the incoming ram pressure. Two additional viability requirements arise within the settling layer: the base pressure must be sufficient to match the post-shock pressure, and the atmosphere must be optically thick across a local scale height so that diffusion is

self-consistent. For sub-Eddington supply the optical-thickness requirement typically provides the more restrictive lower bound on the base temperature; making the shock-support bound dominant would require an extreme redshift hierarchy between the foil and the emitting photosphere.

For compact surfaces the solutions exhibit a clean scale separation: the redshifted temperature varies only weakly across the layer while the density decreases rapidly (more slowly than a simple exponential in the natural near-horizon height coordinate). The physical thickness of the atmosphere shrinks as the surface becomes more compact. A relativistic enthalpy correction can modify the immediate base behavior only at ultra-relativistic baryon temperatures (well above those relevant for the applications of interest); in the parameter regime considered here the layer remains pressure supported, convectively stable, and globally subsonic.

Because the relevant Killing energy current is conserved, the luminosity measured at infinity is radius independent throughout the atmosphere. Consequently, in the optically thick diffusion dominated regime the emergent photosphere luminosity is driven close to the accretion power processed through the layer, largely independent of the foil redshift. Within the assumptions adopted here (steady state, spherical symmetry, local surface interactions, and diffusive transport in an optically thick scattering atmosphere), redshift and diffusion do not provide a generic mechanism to hide accretion power from distant observers.

Finally, the microphysics of gas-surface interaction imposes an additional local constraint at the base: gas-surface collisions and conductive transport produce an effective floor on the base gas temperature that depends on the accommodation efficiency and the ratio of microscopic mean free paths, together with the luminosity crossing the base. This replaces the assumption of an arbitrary base temperature with a controlled, local boundary condition.

Effects beyond the present scope (rotation, magnetic stresses, departures from spherical symmetry, and composition-dependent opacities) can be incorporated as extensions. While these can change detailed profiles and the location of the photosphere, they are not expected to alter the central conservation argument that ties the emergent luminosity to the accretion power in optically thick settling layers.

<sup>1</sup> This work was supported in part by Perimeter Institute  
<sup>2</sup> for Theoretical Physics and the University of Waterloo.  
<sup>3</sup> Research at Perimeter Institute is supported by the  
<sup>4</sup> Government of Canada through the Department of Innovation,  
<sup>5</sup> Science and Economic Development Canada and  
<sup>6</sup> by the Province of Ontario through the Ministry of Eco-  
<sup>7</sup> nomic Development, Job Creation and Trade. A.E.B.  
<sup>8</sup> receives additional financial support from the Natural  
<sup>9</sup> Sciences and Engineering Research Council of Canada  
<sup>10</sup> through a Discovery Grant.

## APPENDIX

### A. OPTICAL THICKNESS AND THE TRANSPORT OPACITY

The relativistic diffusion closure adopted in this work applies when the photon mean free path is small in comparison to the scales on which the thermodynamic variables vary. In a thin, pressure supported settling layer the relevant length is the local (proper) scale height  $H$ , not the global accretion flow size. Accordingly we take the basic requirement for diffusion to be a transport optical depth across a scale height,

$$\tau_H \equiv \int \kappa_R \rho d\ell \sim \kappa_R \rho H \gtrsim 1, \quad (\text{A1})$$

where  $\kappa_R$  is the Rosseland mean transport opacity (absorption+scattering). This condition is stronger than merely having a large total path length: it guarantees the mean free path is short compared to the gradient scale so that the flux can be written in local diffusive form. If scattering dominates,  $\tau_H \gg 1$  ensures trapping and diffusion, while exact LTE/blackbody formation is controlled by an effective absorption depth.

#### A.1. Why a settling layer tends to be optically thick.

A key point is that in a slow settling atmosphere the optical depth is controlled by the residence time of accreted baryons in the layer. The column density in the atmosphere is, parametrically,

$$\Sigma \sim \frac{\dot{M} t_{\text{set}}}{4\pi r_f^2}, \quad t_{\text{set}} \sim \frac{H}{|v_r|}, \quad (\text{A2})$$

so  $\tau_H \sim \kappa_R \Sigma$ . In the subsonic settling regime the drift speed is bounded by a thermal speed at the base; with our kinetic wall closure one has  $|v_r|_f \sim |\mathcal{T}| c_s(T_f)$  with  $c_s^2 \equiv kT/m$ . Hydrostatic support gives  $H \sim c_s^2/|g|$ . Combining these scalings yields

$$\begin{aligned} \tau_H &\sim \kappa_R \frac{\dot{M}}{4\pi r_f^2} \frac{c_s}{|\mathcal{T}| |g|} \\ &\Rightarrow \tau_H \sim \frac{\kappa_R}{\kappa_{\text{es}}} \frac{L_{\text{eq}}}{L_{\text{Edd}}} \frac{c_s(T_f)}{\eta |\mathcal{T}| c}, \end{aligned} \quad (\text{A3})$$

where  $L_{\text{eq}} \equiv \eta \dot{M} c^2$  is the accretion power available at the photosphere/shock and  $L_{\text{Edd}} \equiv 4\pi GMc/\kappa_{\text{es}}$  is the Eddington luminosity correspond to the same transport opacity. Equation A3 makes the physics transparent: for fixed accretion supply, the transport depth grows in direct proportion to the time it takes the surface to process baryons. If  $\kappa_R = \kappa_{\text{es}}$ , then for sufficiently small  $\mathcal{T}$ ,  $\tau_H \gg 1$  and the settling atmosphere is optically thick.

However, the dominant absorption process need not be electron scattering, i.e.,  $\kappa_R$  can differ from  $\kappa_{\text{es}}$ . If absorption in the impinging accretion flow is dominated by synchrotron self-absorption (SSA), as is the case in Sgr A\* and M87\*, then  $\kappa_R$  (the relevant Rosseland mean) can greatly exceed  $\kappa_{\text{es}}$  by many orders of magnitude.

SSA requires a magnetized plasma and a population of relativistic electrons, both of which are naturally supplied by the accretion flow and shock acceleration; upon compression in the surface layer,  $n_e$  and  $B$  increase, further enhancing the SSA optical depth. In our treatment the magnetic field is introduced only as a radiative ingredient (entering  $\kappa_R$ ), and need not be dynamically important. Nevertheless, if magnetic fields are dynamically important, their added pressure support would tend to increase the scale height/column and thus increase the optical depth.

Even when the upstream flow is optically thin at near-IR frequencies, those that dominate the thermal emission at  $T_{\text{eq}}$  for Sgr A\* and M87\*, the accumulated settling layer can become optically thick because synchrotron absorption depends steeply on density. For a power-law electron distribution  $N(\gamma) \propto \gamma^{-p}$  with optically thin index  $\alpha = (p-1)/2$ , synchrotron self-

absorption gives the scaling

$$\rho\kappa_\nu \equiv \alpha_\nu \propto n_e B^{\alpha+3/2} \nu^{-(\alpha+5/2)}. \quad (\text{A4})$$

With  $n_e \propto \rho$  and flux-frozen isotropic compression  $B \propto \rho^{2/3}$ , this becomes

$$\alpha_\nu \propto \rho^{2+\frac{2}{3}\alpha} \nu^{-(\alpha+5/2)}. \quad (\text{A5})$$

Thus, while the high frequency optical depth is suppressed relative to mm by the factor  $(\nu_{\text{NIR}}/\nu_{\text{mm}})^{-(\alpha+5/2)}$ , even a modest density amplification in the settling atmosphere can overwhelm this penalty. For example, taking  $\alpha \simeq 1.25$  and  $\nu_{\text{NIR}}/\nu_{\text{mm}} \sim 10^3$  gives a frequency suppression  $\sim 10^{-11}$ , whereas a density contrast  $\rho_{\text{atm}}/\rho_{\text{acc}} \sim 10^9$  boosts  $\alpha_\nu$  by  $(10^9)^{2+\frac{2}{3}\alpha} \sim 10^{25}$ .

Low-luminosity black hole systems (e.g., Sgr A\* and M87\*) are observed to sit near the synchrotron self-absorption turnover at mm wavelengths. In EHT-motivated one-zone spectral models, the synchrotron optical depth at 230 GHz are of order unity, with representative values  $\tau_{230} \sim 0.4$  for Sgr A\* and  $\tau_{230} \sim 0.2$  for M87\* (depending on model assumptions and position across the image) [Event Horizon Telescope Collaboration et al. \(2019c, 2022c\)](#). Broadband analyses likewise indicate that frequencies below  $\sim 230$  GHz are typically SSA-thick in the inner M87 system [Algaba et al. \(2024\)](#). Taken together, these constraints motivate using  $\tau_{\text{mm}} = \mathcal{O}(0.1\text{-}1)$ ; the steep density dependence in [Equation A4](#) and [Equation A5](#) then implies that a modest increase in column and field strength in the settling layer can drive  $\tau_\nu$  to order unity or larger even when the upstream flow is optically thin at higher frequencies.

### A.2. Angle-dependent optical depth.

Up to this point we have implicitly characterized the layer by its vertical (radial) optical depth across a scale height,  $\tau_\perp \sim \kappa_R \rho H$ . However, a geometrically thin layer is strongly anisotropic: its thickness is  $\sim H$ , while its lateral extent is  $\sim R$ . Consequently, radiative transfer depends sharply on direction. In a plane parallel approximation, a ray emitted at angle  $\theta$  to the local normal traverses a slant column larger by  $1/\mu$  with  $\mu \equiv \cos \theta$ , so that

$$\tau(\mu) \simeq \frac{\tau_\perp}{\mu}. \quad (\text{A6})$$

Even when  $\tau_\perp \lesssim 1$ , a wide range of shallow-angle trajectories can have  $\tau(\mu) \gg 1$ , leading to repeated scattering/absorption and substantial radiative redistribution along the surface. Therefore, the layer can behave optically thick to much of its own emission even if it is only marginally thick in the vertical direction.

### A.3. Strong field escape geometry.

The discussion above is purely geometrical and does not invoke gravity. Gravitational lensing can further

increase surface self-irradiation by bending trajectories back toward the surface and increasing the number of surface reintersections, but this effect is conceptually distinct: it modifies the path topology, whereas the plane parallel argument above already implies strong angle-dependent transfer in a thin, laterally extended layer. In fact, near a highly compact surface, non-radial null geodesics reduce the escape solid angle: only a narrow cone of directions reaches future null infinity, while most trajectories re-intersect the atmosphere due to the photon sphere geometry.

However, gravitational lensing is not expected to alter the local diffusive closure in the optically thick interior.

### A.4. Scope and special cases.

The diffusion solutions apply to optically thick settling layers with  $\tau \equiv \kappa_R P/|g| \gtrsim 1$  and  $\kappa_R \simeq \kappa_{\text{es}}$ . One can, however, envision parameter choices for which the accumulated layer remains optically thin ( $\tau \lesssim 1$ ), e.g., at extremely low  $M$ , or if the surface processes baryons nearly as fast as they arrive (near-maximal  $|\mathcal{T}| \rightarrow 1$ , preventing column build-up) then the appropriate closure is optically thin / flux-limited transport rather than diffusion. Likewise, ultra-strong magnetic fields ( $B \gtrsim 10^8$  G) that shift cyclotron/synchrotron absorption into the Roseland band would require frequency-dependent transfer and a revised  $\kappa_R$ . These regimes lie outside the framework considered here.

## B. RELAXING THE SLOW SETTLING ASSUMPTION: TRANSONIC INNER SOLUTIONS

This section extends the steady, spherical atmosphere to allow an inner transonic transition. We retain the relativistic framework, Thomson opacity, and radiative diffusion used in the main text. The only change is that we no longer assume  $|u^r| \ll c$  at the base: the flow may cross the sonic point once on the way to the foil. What changes in the transonic case is the treatment of the critical point where the sonic denominator vanishes.

### B.1. Equations of motion

We keep the same barred variables as in the main text. The luminosity measured at infinity  $L_\infty$  remains radially conserved by the Killing energy current ( $\nabla_\mu T^{\mu\nu} = 0$ ). With gas pressure dominant (radiation pressure not included here), the steady, spherically symmetric system continuity, Euler, and diffusion respectfully reads as in the main text, since the slow settling assumption is not used and no additional approximations are introduced in them.

### B.2. Mach number and sonic condition

The denominator in  $\partial_s \bar{x}$ , [Equation 56](#), plays the role of  $c_s^2 - v^2$ . This motivates the (barred) Mach number

$$\mathcal{M}^2(s) \equiv \left(\frac{N}{N_f}\right)^3 \frac{\mathcal{T}^2 \bar{y}_f}{\bar{x}^2 \bar{y}}, \quad (\text{B7})$$

Therefore

$$\mathcal{M} = 1 \iff \text{sonic.} \quad (\text{B8})$$

A regular transonic solution that crosses  $\mathcal{M} = 1$  at the sonic point must satisfy two critical conditions. Let the sonic point be at  $r = r_*$ :

1. Sonic condition:

$$\bar{y}_* = \left( \frac{N_*}{N_f} \right)^3 \frac{\mathcal{T}^2 \bar{y}_f}{\bar{x}_*^2}, \quad (\text{B9})$$

2. Regularity (finite slope, i.e, numerator of [Equation 56](#) vanishes):

$$-\frac{N_f}{N_*} \frac{1}{c^2} + \frac{3 \bar{y}_* y_{\text{eq}}}{c^2} \frac{N_f}{N_*^2} + \frac{3 \tau_h N_f^2}{4} \frac{L_\infty}{L_{\text{eq}}} \frac{1}{N_*} \frac{\bar{x}_*}{\bar{y}_*^3} = 0, \quad (\text{B10})$$

where  $y_{\text{eq}} = kT_{\text{eq}}/m$ ,  $\tau_h = \kappa \rho_f h$ , and  $L_{\text{eq}} = 4\pi r_s^2 \sigma T_{\text{eq}}^4 = \eta \dot{M} c^2$ . Using the temperature equation [Equation 66](#), the regularity condition [Equation B10](#) can be written compactly as

$$-\frac{N_f}{N_*} \frac{1}{c^2} + \frac{3 \bar{y}_* y_{\text{eq}}}{c^2} \frac{N_f}{N_*^2} - (\partial_s \bar{y}) = 0. \quad (\text{B11})$$

It means the enthalpy-gravity balance equals the local temperature rise. This gives the finite slopes

$$(\partial_s \bar{y})|_* = \frac{N_f}{c^2} \left( -\frac{1}{N_*} + 3 \frac{y_{\text{eq}} \bar{y}_*}{N_*^2} \right), \quad (\text{B12})$$

$$\frac{\partial_s \bar{x}}{\bar{x}} \Big|_* = \frac{3}{2} \frac{\partial_s N}{N} \Big|_* - \frac{1}{2} \frac{\partial_s \bar{y}}{\bar{y}} \Big|_* = \frac{N_f}{2 c^2 N_* \bar{y}_*}. \quad (\text{B13})$$

In Schwarzschild and within the thin-layer approximation,  $\partial_s \ln N \simeq (y_{\text{eq}}/c^2) N_f/N^2$ , so [Equation B13](#) is already fully explicit once  $\bar{y}_*$  is chosen and  $\bar{x}_*$  is set by [Equation B9](#). These two relations provide a numerically stable initializer for integrating [Equation 56](#) inward/outward through  $r_*$ .

For accretion powered layers one has  $L_\infty \leq 0$ , hence  $\partial_s \bar{y} > 0$ . Since  $N$  increases outward, [Equation B11](#) implies

$$\frac{3 \bar{y}_* y_{\text{eq}}}{c^2} \frac{N_f}{N_*^2} > \frac{N_f}{N_*} \frac{1}{c^2} \implies 3 \frac{kT_*}{mc^2} > 1. \quad (\text{B14})$$

This cleanly explains why transonic solutions are irrelevant in the baryonic temperature regime of interest. Thus a smooth sonic transition would require  $kT_* > mc^2/3$ , i.e. ultra-relativistic baryon temperatures at the sonic point (for protons,  $T_* \gtrsim 3 \times 10^{12}$  K), well above the regime of interest in the main text. Practically, the solutions remain subsonic; any attempted acceleration would require an inner shock to connect to the solid surface (if a surface is to be reached).

### B.3. Inner boundary and microphysics

Two remarks are important at the foil  $r = r_f$ :

i) Mass flux. In the subsonic model we we imposed a kinetic inflow  $J = N_f r_f^2 \mathcal{T} \rho_f \sqrt{kT_f/m}$ , [Equation 59](#). Here the  $N_f$  converts proper to coordinate time and  $\mathcal{T}$  parameterizes the wall transmittance relative to a thermal impingement rate. Once the flow becomes transonic/supersonic at  $r_f$ , this linear subsonic ansatz is no longer appropriate as a constraint. In the transonic extension we instead take the mass flux directly from continuity,  $J = r_f^2 \rho_f u_f^r$  and regard the transmittance as a diagnostic of how absorptive the surface is, rather than a limiter. A convenient diagnostic is the effective transmittance

$$\mathcal{T}_{\text{eff}} \equiv \frac{u_f^r}{N_f \sqrt{kT_f/m}}, \quad (\text{B15})$$

which reproduces the subsonic boundary law when  $|\mathcal{T}_{\text{eff}}| \ll 1$  and reduces to continuity in general<sup>7</sup>.

ii) Temperature boundary condition. The microphysical base condition from wall-gas interaction (see [Section 5.2](#)) is local and unaffected by the Mach number; it only involves the diffusive/conductive flux and the kinetic energy accommodation at the wall. Thus, Equations of microphysics boundary conditions remain unchanged.

### B.4. Summary and Consequences

Given  $(\mathcal{T}, L_\infty)$ , choose a trial sonic location  $s_*$  and solve the sonic condition [Equation B9](#) together with the regularity condition [Equation B10](#) for  $(\bar{x}_*, \bar{y}_*)$ . The corresponding finite derivatives at the sonic point are then obtained from the temperature equation as written in [Equation B11](#) and, equivalently, by the explicit relations [Equation B12](#)-[Equation B13](#). These provide a regular eigenslope initializer for integrating the system of [Equation 56](#) and [Equation 66](#) together, both inward and outward through  $r_*$ .

In the parameter space relevant here, the necessary temperature criterion for a smooth crossing,  $3kT_*/m > 1$ , is not satisfied. Consequently, no global, regular transonic solution exists under the assumptions of the main text (gas pressure support, gray diffusion, steady, spherical flow).

Practically, allowing a transonic inner region mainly reshapes the density profile near the foil: the atmosphere may accelerate and thin close to the surface, terminating in a thin shock or boundary layer, but the global energetics are unchanged.

<sup>7</sup> No bound like  $|\mathcal{T}| < 1$  is imposed in the transonic case; regularity is instead enforced by the sonic conditions (see [Appendix B](#)).

To sum up, (i) the luminosity measured at infinity,  $L_\infty$ , is radially conserved by the Killing energy current, so the emergent power is set by the accretion power processed through the layer; and (ii) with  $L_\infty < 0$  the redshifted temperature  $T_\infty$  still increases outward, so the layer implying convective stability. In practice, the transonic region is narrow for the cool, optically thick atmospheres considered here; it primarily changes the inner matching to the foil rather than the conserved luminosity result.

### C. INCLUDING RADIATION PRESSURE AND RADIATIVE INERTIA AT HIGH $L/L_{\text{EDD}}$

This section consider a minimal, self-consistent relativistic upgrade of the settling layer equations that accounts for radiation pressure and radiative inertia when the luminosity approaches the Eddington scale. We keep the steady, spherical, subsonic assumptions and the diffusion closure; the only new ingredients are (i) the radiation contribution to pressure and inertia and (ii) the reduction of effective gravity by the (radius-independent) Eddington factor. The aim is to show where the terms enter and how the equations are modified, without altering the structure of the main text.

#### C.1. Total stress energy and basic definitions

We split the total stress energy into gas and radiation,

$$T^{\mu\nu} = T_g^{\mu\nu} + R^{\mu\nu}. \quad (\text{C16})$$

For the gas we use the perfect fluid form  $T_g^{\mu\nu} = (\varepsilon_g + P_g)u^\mu u^\nu + P_g g^{\mu\nu}$  (with  $\varepsilon_g \simeq \rho c^2$  in our atmosphere). In the comoving (fluid) frame and in the diffusion limit with Thomson scattering, the radiation moments are

$$E_{\text{rad}} = aT^4, \quad P_{\text{rad}} = \frac{1}{3}aT^4, \quad F^\mu. \quad (\text{C17})$$

Here  $F^\mu$  is first order in gradients, and  $R^{\mu\nu}$  has the usual  $(E_{\text{rad}}, P_{\text{rad}}, F^\mu)$  structure.

We use the same barred variables as in the main text

$$\bar{x}(r) \equiv \frac{N(r)^2 \rho(r)}{N_f^2 \rho_f}, \quad \bar{y}(r) \equiv \frac{N(r) T(r)}{T_{\text{eq}}}, \quad (\text{C18})$$

where  $y_{\text{eq}}$  is given by Equation 54, and  $N(r) = \sqrt{1 - 2GM/(rc^2)}$ , and the subscript  $f$  denotes the base ( $r = r_f$ ). In terms of  $\bar{x}, \bar{y}$  the physical fields are

$$\rho(r) = \frac{N_f^2 \rho_f}{N(r)^2} \bar{x}(r), \quad T(r) = \frac{T_{\text{eq}}}{N(r)} \bar{y}(r). \quad (\text{C19})$$

The gas pressure is

$$P_g(r) = \rho \frac{kT}{m} = \frac{N_f^2 \rho_f y_{\text{eq}}}{N(r)^3} \bar{x}(r) \bar{y}(r). \quad (\text{C20})$$

The radiation pressure is

$$P_{\text{rad}}(r) = \frac{1}{3}aT^4 = \frac{a}{3}T_{\text{eq}}^4 \frac{\bar{y}(r)^4}{N(r)^4}. \quad (\text{C21})$$

(We will also use  $E_{\text{rad}} = 3P_{\text{rad}}$  from the radiation moments.) Radiation contributes to the inertia through  $(E_{\text{rad}} + P_{\text{rad}})/c^2 = 4P_{\text{rad}}/c^2$ . Neglecting the small gas-enthalpy term  $P_g/c^2$  (since  $kT \ll mc^2$  in the layer), the effective inertia entering the Euler equation is

$$\begin{aligned} \rho_{\text{eff}}(r) &\equiv \rho(r) + \frac{4}{c^2} P_{\text{rad}}(r) \\ &= \frac{N_f^2 \rho_f}{N(r)^2} \bar{x}(r) + \frac{4a}{3c^2} T_{\text{eq}}^4 \frac{\bar{y}(r)^4}{N(r)}. \end{aligned} \quad (\text{C22})$$

For Eddington factor; For gray scattering the relativistic Eddington ratio

$$\Gamma \equiv \frac{\kappa L_\infty}{4\pi G M c}, \quad (\text{C23})$$

is radius-independent (because  $L_\infty$  is conserved along  $r$ ). In the radial Euler equation the radiative force density  $(\kappa\rho/c)F$  can be expressed in terms of  $L_\infty$ ,

In Schwarzschild, including both radiative inertia and the scattering force, the combination of gravity and radiative driving enters through the single factor  $\rho_{\text{eff}} - \Gamma\rho$  in the term proportional to  $\partial_r \ln N^2$ . In the gas-dominated inertia limit ( $P_{\text{rad}} \ll \rho c^2$  so that  $\rho_{\text{eff}} \simeq \rho$ ) this reduces to the familiar  $(1 - \Gamma)$  reduction.

#### C.2. Conservation laws and luminosity

Total conservation  $\nabla_\nu T^{\mu\nu} = 0$  still implies a conserved energy current  $J^\mu \equiv -T^\mu_\nu k^\nu$  associated with the timelike Killing vector  $k^\nu = \partial_t$ . As in the main text,

$$L_\infty(r) = \int_{S_r} J^\mu d\Sigma_\mu, \quad (\text{C24})$$

is independent of  $r$ . In other words, the luminosity measured at infinity is the same whether evaluated at the base (from the diffusive flux) or at the top (from the thermal emission). None of the manipulations below modify this fact.

#### C.3. Continuity and diffusion: forms unchanged

*Continuity.*—Spherical steady flow gives

$$\frac{1}{r^2} \partial_r(r^2 \rho u^r) = 0 \iff J \equiv -r^2 \rho u^r = \text{const.} \quad (\text{C25})$$

identical to the main text.

*Diffusion (for  $T_\infty$ ).*—The relativistic diffusion law derived in the main text Equation 51 carries over

$$\partial_r T_\infty = -\frac{3\kappa\rho N}{64\pi r^2 \sigma T_\infty^3} L_\infty, \quad T_\infty \equiv NT. \quad (\text{C26})$$

Thomson scattering fixes the mean free path  $\lambda = (\kappa\rho)^{-1}$ , so radiation pressure/inertia does not alter the transport coefficient itself (if true absorption at the Rosseland peak becomes important, one replaces  $\kappa$  by  $\kappa_R$  everywhere; the derivation is otherwise identical).

#### C.4. Euler with radiation pressure and radiative inertia

Projecting  $\nabla_\nu T^{\mu\nu} = 0$  orthogonally to  $u^\mu$  yields the radial momentum equation. In steady spherical symmetry one may write it in two equivalent ways.

(i) Total fluid form. Grouping gas and radiation into a single effective fluid gives

$$\rho_{\text{eff}} u^r \partial_r u_r = -\partial_r P_{\text{tot}} - \frac{1}{2} (\rho_{\text{eff}} - \Gamma \rho) \partial_r \ln(N^2),$$

$$P_{\text{tot}} \equiv P_{\text{g}} + P_{\text{rad}}, \quad (\text{C27})$$

with  $\rho_{\text{eff}}$  from Equation C22 and  $\Gamma$  from Equation C23.

(ii) Gas plus force form. Alternatively, one may keep the gas inertia on the left and treat the radiation as a force density on the right,

$$\rho u^r \partial_r u_r = -\partial_r P_{\text{g}} - \frac{1}{2} \rho \partial_r \ln(N^2) + \underbrace{\frac{\kappa \rho}{c} F_{\hat{r}}}_{\text{radiative force}}$$

$$- \partial_r P_{\text{rad}} - \frac{1}{2} \frac{4P_{\text{rad}}}{c^2} \partial_r \ln(N^2). \quad (\text{C28})$$

Here  $F_{\hat{r}}$  is the local (orthonormal) radiative flux measured by static observers. Using the Killing energy conservation and the Schwarzschild redshift one may show  $F_{\hat{r}} = L_\infty / (4\pi N^2 r^2)$  and the radiative acceleration is  $\kappa \rho F_{\hat{r}} / c = (1/2) \Gamma \rho \partial_r \ln(N^2)$ ; insertion of these identities converts Equation C28 into Equation C27. However, we use Equation C27 below because it keeps the structure of the main text intact.

In fact, for  $\Gamma \rightarrow 0$  and  $P_{\text{rad}} \rightarrow 0$  the system reduces exactly to the gas only equations in the main text. In the static limit  $u^r = 0$  one recovers the relativistic hydrostatic balance with radiation

$$\frac{dP_{\text{tot}}}{dr} = -\frac{1}{2} (\rho_{\text{eff}} - \Gamma \rho) \frac{d \ln N^2}{dr}. \quad (\text{C29})$$

In the weak-field (Newtonian) limit identifying the mass density  $\rho_N \equiv \rho / c^2$ , the equations reduce to the familiar

$$\frac{d(P_{\text{g}} + P_{\text{rad}})}{dr} = -\rho_N g (1 - \Gamma) \equiv -\rho_N g_{\text{eff}}, \quad (\text{C30})$$

Therefore, the Eddington reduction multiplies the gravitational term while radiative inertia drops out of static balance at leading order. The Killing-energy current  $J^\mu = -T^{\mu\nu} k_\nu$  remains conserved, so the luminosity conservation proof and  $L_\infty = \text{const}$  are unaffected by the inclusion of radiation pressure and inertia..

#### C.5. Sonic discriminant (effective sound speed)

It is convenient to define

$$\wp(\bar{x}, \bar{y}; N) \equiv \frac{4P_{\text{rad}}}{\rho c^2} = \frac{4a}{3c^2} \frac{T_{\text{eq}}^4}{N_f^2 \rho_f} \frac{\bar{y}^4}{N^2 \bar{x}}, \quad (\text{C31})$$

and the effective inertia Equation C22 becomes

$$\rho_{\text{eff}} = \rho (1 + \wp). \quad (\text{C32})$$

In the relativistic ODE the sonic denominator Equation 63, comes from the balance of the pressure's response (sound speed piece) against the kinematic term  $J^2 / (N \rho^2 r^4)$  generated when eliminating the velocity in favor of  $J$ . To capture radiative inertia in the same rationalized ODE structure, we model its effect on the sonic discriminant by the substitution  $y_{\text{eq}} \bar{y} \mapsto y_{\text{eq}} \bar{y} (1 + \wp)$ , i.e. by treating  $\rho_{\text{eff}} = \rho (1 + \wp)$  as an effective enhancement of the pressure response term.

$$\underbrace{y_{\text{eq}} \bar{y}}_{\text{gas } c_s^2} \implies \underbrace{y_{\text{eq}} \bar{y} (1 + \wp)}_{\text{gas + radiative inertia}}, \quad (\text{C33})$$

hence at the base  $r = r_f$  the subsonic base condition Equation 65 becomes

$$1 + \wp_f - \mathcal{T}^2 > 0 \iff |\mathcal{T}| < \sqrt{1 + \wp_f}, \quad (\text{C34})$$

which reduces to  $|\mathcal{T}| < 1$  when  $\wp_f \ll 1$ .

#### C.6. Boundary data and checks

*Top boundary (photosphere / shock interface).*—The normal stress balance across the interface at  $r = r_s$  should include radiation pressure on whichever side it is dynamically important. With a subsonic base on the atmospheric side ( $u^r(r_s) \simeq 0$ ), one has

$$P_{\text{tot},s} \equiv P_{\text{g},s} + P_{\text{rad},s} = \frac{N_f^2 \rho_f y_{\text{eq}}}{N_s^3} \bar{x}_s \bar{y}_s + \frac{a}{3} \frac{T_{\text{eq}}^4}{N_s^4} \bar{y}_s^4$$

$$\simeq \underbrace{\frac{\rho_a (u_a^r)^2}{N_s^2} + P_a + P_{\text{rad},a}}_{\text{upstream}}, \quad (\text{C35})$$

where the upstream (accretion) side may be simplified to  $P_{\text{rad},a} \approx 0$ ,  $P_a \approx 0$  for a cold, hypersonic inflow, and  $\rho_a u_a^r = \dot{M} / (4\pi r_s^2)$  by continuity. If upstream dissipation reduces the impact speed, write  $u_a^r = \eta_{\text{ram}} c$  to obtain

$$\frac{N_f^2 \rho_f y_{\text{eq}}}{N_s^3} \bar{x}_s \bar{y}_s + \frac{a}{3} \frac{T_{\text{eq}}^4}{N_s^4} \bar{y}_s^4 \simeq \eta_{\text{ram}} \frac{\dot{M} c}{4\pi r_s^2 N_s^2}. \quad (\text{C36})$$

In the regime where  $P_{\text{rad},s} \ll P_{\text{g},s}$ , Equation C36 reduce to the gas-only matching used in the main text (with  $\eta_{\text{ram}}$  identified with  $\eta$  under the same assumptions). The energy balance that sets  $L_\infty$  is unchanged

$$L_\infty = \frac{4\pi r_s^2}{N_s^2} \sigma T_{\infty,s}^4 - \eta \dot{M} c^2 = L_{\text{eq}} (\bar{y}_s^4 - 1), \quad (\text{C37})$$

where  $T_{\infty,s} = T_{\text{eq}} \bar{y}_s$ . Since it follows from Killing-energy conservation; radiation pressure only enters through  $P_{\text{tot}}$  in the stress balance, not in Equation C37.

*Microscopic base boundary.*—The kinetic wall boundary that fixes  $T_f$  is local and occurs across a layer of thickness  $\lambda_c \ll h$ . Over this microscopic scale the lapse is constant to excellent approximation ( $N \simeq N_f$ ), so the relativistic redshift factors drop out and the derivation of the temperature floor proceeds exactly as in the main text.

### C.7. Validity of the diffusion equation near the photosphere

In a local orthonormal (hat) frame comoving with the static observers, let  $E$  be the radiation energy density,  $F_{\hat{r}}$  the radial flux, and  $P_{\hat{r}\hat{r}}$  the radial radiation pressure. They are the first angular moments of the specific intensity. Causality bounds  $|F_{\hat{r}}| \leq cE$ . It is convenient to define the reduced flux

$$f \equiv \frac{|F_{\hat{r}}|}{cE} \in [0, 1], \quad E = aT^4, \quad a = \frac{4\sigma}{c}. \quad (\text{C38})$$

The field is nearly isotropic when  $f \ll 1$  and free streaming when  $f \rightarrow 1$ .

For Thomson opacity  $\kappa$  and mean free path  $\lambda = (\kappa\rho)^{-1}$ , the diffusion limit (large optical depth  $\tau \equiv \ell/\lambda \gg 1$ ) gives

$$\begin{aligned} F_{\hat{r}} &\simeq -\frac{c}{3\kappa\rho} \frac{dE}{d\ell} \\ \Rightarrow f &\simeq \frac{|F_{\hat{r}}|}{cE} \simeq \frac{1}{3} \frac{\lambda}{\ell} = \frac{1}{3\tau} \ll 1, \end{aligned} \quad (\text{C39})$$

where  $\ell \equiv E/|dE/d\ell|$  is the local gradient scale. In this regime, using  $E = aT^4$  and the GR redshift bookkeeping ( $d\ell = dr/N$ ,  $T_\infty \equiv NT$ ) (Section 4.3) yields the diffusion equation we used in the main text, Equation 51,

$$\partial_r T_\infty = -\frac{3\kappa\rho N}{64\pi r^2\sigma T_\infty^3} L_\infty, \quad T_\infty \equiv NT. \quad (\text{C40})$$

If  $f$  approaches unity; near the photosphere, the 1/3 Eddington factor is no longer accurate. Two standard upgrades preserve causality and smoothly connect diffusion to streaming, without changing the global conservation of Killing energy  $L_\infty$ .

1. Flux limited diffusion (FLD). Keep a diffusion type law but limit the coefficient:

$$F_{\hat{r}} = -\frac{c\lambda_{\text{FL}}(R)}{\kappa\rho} \frac{dE}{d\ell}, \quad R \equiv \frac{1}{\kappa\rho} \frac{|dE/d\ell|}{E}, \quad (\text{C41})$$

with the flux limiter  $\lambda_{\text{FL}}(R)$  chosen so that  $\lambda_{\text{FL}} \rightarrow 1/3$  for  $R \ll 1$  (diffusion) and  $\lambda_{\text{FL}} \rightarrow 1/R$  for  $R \gg 1$  (free streaming), which enforces  $f = \lambda_{\text{FL}}R \leq 1$ . A common analytic choice is Levermore-Pomraning (see e.g., Levermore (1984)):  $\lambda_{\text{FL}}(R) = \frac{1}{R}(\coth R - \frac{1}{R})$ . In our spherical, steady setting this amounts to replacing the

factor 1/3 by  $\lambda_{\text{FL}}$  in the conductivity, i.e.

$$\partial_r T_\infty = -\frac{\kappa\rho N}{64\pi r^2\sigma T_\infty^3} \frac{1}{\lambda_{\text{FL}}(R)} L_\infty, \quad (\text{C42})$$

which reduces to Equation 51 when  $\lambda_{\text{FL}} = 1/3$ .

2. two-moment closure (M1). Evolve two moments  $(E, F_{\hat{r}})$  and close the pressure tensor with an Eddington factor that depends on  $f$

$$P_{\hat{r}\hat{r}} = \chi(f) E, \quad \chi(f) = \frac{3 + 4f^2}{5 + 2\sqrt{4 - 3f^2}}, \quad (\text{C43})$$

so  $\chi \rightarrow 1/3$  as  $f \rightarrow 0$  and  $\chi \rightarrow 1$  as  $f \rightarrow 1$ . In curved spacetime all relations are evaluated in the local orthonormal frame;  $F_{\hat{r}}$  is tied to  $L_\infty$  by  $L_\infty = 4\pi r^2 N^2 F_{\hat{r}}$ , and the moment equations couple to the gas through  $\kappa$  exactly as in diffusion.

Both FLD and M1 change only the constitutive relation between the local radiation flux/pressure and gradients. The global conserved current  $J^\mu \equiv -T^{\mu\nu} k^\nu$  (with  $T^{\mu\nu}$  the total gas+radiation stress energy and  $k^\nu = \partial_t$  the Killing vector) still obeys  $\nabla_\mu J^\mu = 0$  in steady state. Hence

$$L_\infty(r) = \int_{S_r} J^\mu d\Sigma_\mu, \quad (\text{C44})$$

is radius-independent irrespective of whether one uses pure diffusion, FLD, or M1 in the thin transition layer.

### C.8. Summary and Consequences

To include radiation pressure/inertia in practice, one can use the total fluid Euler form with  $P_{\text{tot}} = P_g + P_{\text{rad}}$ ,  $\rho_{\text{eff}} = \rho + 4P_{\text{rad}}/c^2$ , and multiply the gravitational term by  $(1 - \Gamma)$ . The continuity law is unchanged. The temperature equation keeps the same relativistic diffusion structure Equation 51 (by replacing the 1/3 by a flux limiter or the M1 closure only when  $f \ll 1$ ). In the rationalized ODEs this amounts to the replacements  $g \rightarrow g(1 - \Gamma)$ , and  $\bar{y} \rightarrow (1 + \wp)\bar{y}$  (sonic denominator only), with all other terms unchanged. Base and top boundary conditions are as in the main text, with  $P_{\text{rad}}$  included in the normal stress balance where it is dynamically relevant.

To sum up, radiation affects the settling layer in exactly two ways: (i) it reduces the effective weight by the Eddington factor  $g \rightarrow g_{\text{eff}} \equiv g(1 - \Gamma)$  with  $\Gamma = \kappa L_\infty/(4\pi G M c)$ ; and (ii) it adds radiative inertia to the sonic denominator which we model in the rationalized ODE by an effective modification of the sonic discriminant controlled by  $\rho_{\text{eff}} = \rho(1 + \wp)$  with  $\wp \equiv 4P_{\text{rad}}/(\rho c^2) > 0$ . Thus, the sound speed term is multiplied by  $(1 + \wp)$ , which pushes any transonic point inward for fixed thermodynamic state. As  $\Gamma \rightarrow 1$  hydrostatic balance flattens ( $g_{\text{eff}} \rightarrow 0$ ), the density gradient

can weaken, and the layer can become radiation pressure dominated; nevertheless the Killing energy current remains conserved, so the luminosity at infinity is still radius independent:  $L_\infty(r) = \text{const.}$  The diffusion equation Equation C26 remains valid as long as the reduced flux  $f \equiv |F_r|/(cE) \ll 1$ ; if  $f \sim 1$  approaches unity, near the photosphere, a flux-limited (FLD) or M1 moment closure should replace the 1/3 Eddington factor locally, without changing the global conservation  $L_\infty = \text{const.}$

#### D. CLASSICAL DERIVATION OF RADIATIVE DIFFUSION EQUATION

We begin by noting that the temperature as measured at infinity (e.g., a color temperature) is related to that in the comoving frame by the gravitational redshift,  $T_\infty = NT$ . The luminosity of a thermally emitting spherical surface with radius  $r$  as measured at infinity is given by

$$L_\infty(r, T_\infty) = A_\infty(r) \sigma T_\infty^4 = \frac{4\pi r^2}{N^2} \sigma T_\infty^4, \quad (\text{D45})$$

where the apparent emitting surface area,  $A_\infty(r) = 4\pi r^2/N^2$ , is larger by a factor of  $N^{-2}$  due to gravitational lensing.  $T_\infty$  and  $L_\infty$  provide convenient, gauge-invariant definitions of temperature and luminosity in terms that are observationally relevant.

If the emission region is not moving (i.e.,  $u^r = 0$ ), the local emitted flux is  $F = \sigma T^4 = \sigma(T_\infty/N)^4$ , where the factor of  $N$  accounts for the gravitational redshift. Thus, the flux from a spherical surface at radius  $r$  as measured at a location  $r'$  is

$$F(r'; r) = \sigma [T_\infty(r)/N(r')]^4. \quad (\text{D46})$$

Therefore, the net flux through a surface at radius  $r$  between two spherical surfaces located at  $r - \Delta r/2$  and  $r + \Delta r/2$  is

$$\begin{aligned} F_{\text{net}}(r) &= F(r; r - \Delta r/2) - F(r; r + \Delta r/2) \\ &= \frac{\sigma}{N(r)^4} [T_\infty(r - \Delta r/2)^4 - T_\infty(r + \Delta r/2)^4] \\ &\approx -\frac{4\sigma}{N^4} T_\infty^3 \partial_r T_\infty \Delta r, \end{aligned} \quad (\text{D47})$$

where  $N$  and  $T_\infty$  are evaluated at  $r$ .

Within the diffusion approximation, photons random-walk a characteristic proper distance  $\ell \simeq \lambda/3$  per step along the radial direction, where  $\lambda = (\kappa\rho)^{-1}$  is the comoving mean free path and the factor 1/3 is the usual angular average. In Schwarzschild, the proper radial distance is  $d\ell = dr/N$ , so over one step

$$\Delta r \simeq N \ell \simeq \frac{N\lambda}{3}. \quad (\text{D48})$$

Substituting this into the expression above gives

$$\partial_r T_\infty = -\frac{3\kappa\rho}{N} \frac{N^4}{16\sigma N^3} F_{\text{net}}(r). \quad (\text{D49})$$

Finally, using  $A_\infty(r) = 4\pi r^2/N^2$  and  $L_\infty = A_\infty \sigma T_\infty^4$ , the net local flux is related to  $L_\infty$  by

$$N^4 F_{\text{net}}(r) = \frac{N^2}{4\pi r^2} L_\infty. \quad (\text{D50})$$

we have

$$\partial_r T_\infty = -\frac{3\kappa\rho N L_\infty}{64\pi r^2 \sigma T_\infty^3}. \quad (\text{D51})$$

When expressed this way, the radiative diffusion equation matches Equation 51, with the redefinition of  $T$  to be  $T_\infty$  and  $L$  to be  $L_\infty$ , thereby incorporating the gravitational redshift and lensing naturally. We note that when  $L_\infty = 0$ , i.e., the source is in global thermal equilibrium,  $T_\infty$  is constant.

#### REFERENCES

Abac, A. G., Abbott, R., Abouelfettouh, I., et al. 2024, ApJL, 970, L34

Abac, A. G., Abouelfettouh, I., Acernese, F., et al. 2025, PhRvL, 135, 111403

Abbott, B. P., Abbott, R., Abbott, T. D., et al. 2016, PhRvL, 116, 061102

Abbott, R., Abe, H., Acernese, F., et al. 2025, PhRvD, 112, 084080

Algaba, J. C., et al. 2024, *Astronomy & Astrophysics*

Almheiri, A., Marolf, D., Polchinski, J., Stanford, D., & Sully, J. 2013, *Journal of High Energy Physics*, 2013, 18

Arrechea, J., Barceló, C., Carballo-Rubio, R., & Garay, L. J. 2022, *Scientific Reports*, 12, 15958

Barceló, C., Liberati, S., Sonego, S., & Visser, M. 2008, *Phys. Rev. D*, 77, 044032

Barceló, C., Liberati, S., Sonego, S., & Visser, M. 2011, *Journal of High Energy Physics*, 2011, 3

Bena, I., & Warner, N. P. 2007, arXiv e-prints, hep

—. 2025, arXiv e-prints, arXiv:2503.17310

Broderick, A. E., Loeb, A., & Narayan, R. 2009, *ApJ*, 701, 1357

Broderick, A. E., & Narayan, R. 2007, *Classical and Quantum Gravity*, 24, 659

Broderick, A. E., Narayan, R., Kormendy, J., et al. 2015, *ApJ*, 805, 179

Broderick, A. E., & Salehi, K. 2024, *ApJ*, 977, 249

Broderick, A. E., Salehi, K., & Georgiev, B. 2023, *ApJ*, 958, 114

Buchdahl, H. A. 1959, *Physical Review*, 116, 1027

Cardoso, V., & Pani, P. 2019, *Living Reviews in Relativity*, 22, 4

Danielsson, U., & Giri, S. 2021, *PhRvD*, 104, 124086

Event Horizon Telescope Collaboration, et al. 2019a, *ApJL*, 875, L1

—. 2019b, *ApJL*, 875, L6

Event Horizon Telescope Collaboration, Akiyama, K., Alberdi, A., et al. 2019c, *ApJL*, 875, L5

—. 2022a, *ApJL*, 930, L12

—. 2022b, *ApJL*, 930, L17

—. 2022c, *ApJL*, 930, L16

Hawking, S. W. 1976, *Phys. Rev. D*, 14, 2460

Holdom, B., & Ren, J. 2017, *PhRvD*, 95, 084034

Kaup, D. J. 1968, *Physical Review*, 172, 1331

Kippenhahn, R., & Weigert, A. 1994, *Stellar Structure and Evolution*

Kocherlakota, P., Rezzolla, L., Falcke, H., et al. 2021, *PhRvD*, 103, 104047

Levermore, C. D. 1984, *JQSRT*, 31, 149

Liebling, S. L., & Palenzuela, C. 2012, *Living Reviews in Relativity*, 15, 6

Mathur, S. D. 2002, *International Journal of Modern Physics D*, 11, 1537

Mathur, S. D. 2005, *Fortschritte der Physik*, 53, 793

—. 2009, *Classical and Quantum Gravity*, 26, 224001

Mathur, S. D., & Mehta, M. 2024, arXiv e-prints, arXiv:2412.09495

Mazur, P. O., & Mottola, E. 2004, *Proceedings of the National Academy of Sciences*, 101, 9545

McClintock, J. E., Narayan, R., & Rybicki, G. B. 2004, *ApJ*, 615, 402

Misner, C. W., Thorne, K. S., & Wheeler, J. A. 1973, *Gravitation*

Narayan, R., Garcia, M. R., & McClintock, J. E. 1997, *ApJL*, 478, L79

Narayan, R., & Heyl, J. S. 2002, *ApJL*, 574, L139

Narayan, R., & McClintock, J. E. 2008, *NewAR*, 51, 733

Preskill, J. 1992. <https://arxiv.org/abs/hep-th/9209058>

Ruffini, R., & Bonazzola, S. 1969, *Physical Review*, 187, 1767

Skenderis, K., & Taylor, M. 2008, *PhR*, 467, 117

Tolman, R. C. 1934, *Relativity, Thermodynamics and Cosmology* (Oxford: Clarendon Press)

Tolman, R. C., & Ehrenfest, P. 1930, *Physical Review*, 36, 1791

Vieira, R. S. S., & Kluźniak, W. 2023, *MNRAS*, 523, 4615

Visser, M. 2003, *International Journal of Modern Physics D*, 12, 649

Visser, M., & Wiltshire, D. L. 2004, *Classical and Quantum Gravity*, 21, 1135

Warner, N. P. 2019, arXiv e-prints, arXiv:1912.13108